Mechanistic Studies on Arsenic Toxicity in Endothelial Cells

By Jiani Chen

Submitted to the graduate degree program in Pharmacology and Toxicology and the Graduate Faculty of the University of Kansas in partial fulfillment of the requirements for the degree of Master of Science.

Chair: Dr. Honglian Shi

Dr. Rick Dobrowsky

Dr. Nancy Muma

Date Defended: 2 July 2018

The thesis committee for Jiani Chen certifies that this is the approved version of the following thesis:

Mechanistic Studies on Arsenic Toxicity in Endothelial Cells

Chair: Dr. Honglian Shi

Date Approved: 2 July 2018

Abstract

Arsenic is a well-established human toxin. Over 200 million people worldwide are exposed to arsenic, mainly through drinking water. Recently, several epidemiological studies have reported that even low concentrations of arsenic impair neurological functions across a broad age range in human [1]. However, the cellular and molecular mechanisms of arsenic's effect on the central nervous system (CNS) are not well understood. The blood-brain barrier (BBB) is a complex multicellular structure separating the CNS from the systemic circulation and protects the neural tissue from toxins and pathogens. Alterations in the BBB are an important component of pathology in many neurological disorders [2]. Therefore, arsenic may have a toxic impact on the BBB and thus affect the function of CNS. Since brain endothelial cells (BECs) are the major component of the BBB and play important roles in maintaining the functional integrity of brain tissue under toxic exposure, we focused on arsenic-induced alterations in BECs in our study. Previously, our laboratory has reported that reactive oxygen species (ROS) play an important role in an arsenic-induced increase in brain endothelial cell permeability[3]. However, the underlying mechanism of arsenic-induced ROS generation in endothelial cells and how ROS regulate endothelial cell functions are unclear. Mitochondria are considered as the major source of ROS generation in mammalian cells and arsenic-induced mitochondrial dysfunction has been reported in many studies, which suggest that it may be associated with arsenic-induced oxidative stress in endothelial cells (ECs). In addition, autophagy, which is regulated by oxidative stress, plays an important role to control endothelial permeability and maintain redox balance in ECs and it may also be involved in arsenic toxicity in BECs [4].

Here, we studied mitochondrial ROS generation and the role of autophagy in arsenic-induced toxicity in rat brain endothelial (RBE4) cell line. Our results demonstrate that arsenite increased mitochondrial ROS generation and MnSOD expression and decreased mitochondrial bioenergetics (mtBE) in RBE4 cells. In addition, immunoblot analysis of LC-3(Microtubule-associated protein light chain 3) revealed that arsenite induced autophagy in RBE4 cells as observed by the increased expression of LC3-II and the ratio of LC3-II/LC3-I, which were used as autophagy markers in our study. Furthermore, the antioxidants N-acetylcysteine (NAC) and tempol decreased arsenic-induced mitochondrial ROS generation and autophagy. However, only NAC rescued arsenic decreased mtBE and increased monolayer permeability in RBE4 cells. Taken together, our study supported that mitochondrial oxidative stress and ROS-induced autophagy were involved in arsenic toxicity in RBE4 cells. These findings have given us a new insight into the mechanism underlying arsenic-mediated brain vascular dysfunction.

Acknowledgements

First and Foremost, I would like to thank my advisor Dr. Honglian Shi for giving me the opportunity to complete my two-year masters training in his lab and for introducing me to this interesting project. His endless encouragement and helpful discussions helped me to have the confidence to continue my studies and work as a more independent researcher. I learned not only science from him, but also life lessons. I also want to thank for his advice on my future, which is especially precious and thoughtful.

I also would like to express my thanks to my committee members for their support and suggestions. Dr. Rick Dobrowsky has given me a lot of help for using Seahorse instrument and Dr. Nancy Muma is always supportive and encouraging.

In addition, I would like to thank Dr. Justin Douglas at Core Research Resource Labs for helping Mohammed and me on EPR methodology. Also, I want to thank Dr. Zhenyuan You for training me on Oroboros and Seahorse. I would like to give special thanks to my lab member Mohammed for teaching me all the lab skills and providing great suggestions during these two years. I also want to thank Siying Li for her strong support last year. I would also like to thank all my friends at PTX department who has helped me during the past two years and made it a precious memory to me.

Most importantly, I would like to thank my family. Without their love and support, I can never make it so far.

Table of Contents

List of Figures

List of Tables

List of Abbreviations

$^{\bullet}NO$	nitric oxide
$^{\bullet}NO_2$	nitrogen dioxide radical
$^{\bullet}OH$	hydroxyl radical
2-OH-Mito-E+	2-hydroxy-mito-ethidium
3-MA	3-methyladenine
3-MA	3-methyladenine
AJs	adherent junctions
As	Arsenic
BBB	blood-brain barrier
BECs	brain endothelial cells
CMH	1-hydroxy-3-methoxycarbonyl-2,2,5,5-tetramethylpyrrolidine
CNS	center nervous system
CuZnSOD	copper- and zinc-containing SOD
ECs	endothelial cells
FCCP	carbonyl cyanide 4-(trifluoromethoxy) phenylhydrazone

GPx	glutathione peroxidase
GSH	glutathione
H_2O_2	hydrogen peroxide
HO-1	heme-oxygenase I
LC-3	Microtubule-associated protein light chain 3
MnSOD/ SOD2	Manganese-containing SOD
MRC	maximal respiratory capacity
mtBE	mitochondrial bioenergetics
NAC	N-acetyl-cystine
NO_2^-	nitrite anion
$O_2^{\bullet-}$	superoxide anion
$ONOO^-$	peroxynitrite
PE	phosphatidylethanolamine
PI-3K	Phosphatidylinositol 3-kinase
RBE4	Rat brain endothelial
RNS	reactive nitrogen species

ROS	reactive oxygen species
SOD	superoxide dismutase
Tempol	4-hydroxy-Tempo
TJs	tight junctions
VEGF	vascular endothelial growth factor
WHO	World Health Organization
ZO-1	zonula occludens-1

Chapter 1 Introduction

1.1 Introduction of Arsenic

1.1.1 Arsenic Exposure is a Worldwide Problem

The metalloid arsenic (As) is a natural component of the earth's crust and is widely distributed throughout the environment. Arsenic is found in combination with either inorganic or organic substances to form many different compounds. Inorganic arsenic compounds are found in soils, sediments, and groundwater. These compounds occur naturally or as a result of mining, ore smelting, and industrial use of arsenic. Organic arsenic compounds are found mainly in fish and shellfish which are not known to be toxic to humans. In contrast, inorganic arsenic exposure has been implicated in a variety of health hazards [5]. Acute effects of arsenic range from gastrointestinal distress to death. Depending on its concentration, chronic arsenic exposure can cause cancer, skin lesions, cardiovascular diseases, and neurological impairment [6]. Arsenic holds the highest ranking on the current U.S. Agency for Toxic Substances and Disease Registry (ATSDR) 2017 substance priority list [7].

As mentioned, arsenic is ubiquitous, and humans can be exposed to arsenic via contaminated drinking water, cigarettes, foods, industry, occupational environment, as well as air [8]. Among the various routes of arsenic exposure, arsenic contaminated drinking water is the largest source of arsenic poisoning worldwide [9]. Inorganic arsenic is naturally present at high levels in the groundwater of several countries, including Argentina, Bangladesh, Chile, China, India, Mexico, and the United States of America [8]. It is now

recognized that at least 140 million people in 50 countries have been drinking water containing arsenic at levels above the World Health Organization (WHO) provisional guideline value of 10 μg/L [10]. However, the symptoms and signs that are caused by long-term elevated exposure to inorganic arsenic differ between individuals, population groups and geographical areas. As a result, there is no reliable estimate of the magnitude of the arsenic problem worldwide. Therefore, more research needs to be done to better understand arsenic toxicity.

1.1.2 Arsenic Neurotoxicity

Although the systemic and carcinogenic toxicity of arsenic has been studied in detail, its neurocognitive consequences have not been extensively explored. Recent studies have shown that even at low concentrations, arsenic can impair neurological function [11]. Epidemiological evidence has reported arsenic neurotoxicity in children and adults, with emphasis on cognitive dysfunction, including learning and memory deficits and mood disorders, as well as increased Alzheimer's-associated pathologies (**Table 1.1.2**) [11]. The neurotoxic effects of arsenic have been reported not only in humans but also in many animal models. Arsenic exposure was link to impairments in learning and spatial memory in rodents as determined by poorer performance on hidden platform acquisition tests, novel object exploration as well as the Morris water maze test [1, 12, 13] . In addition, animal studies have demonstrated that prenatal and early postnatal arsenic exposure reduced brain weight, the numbers of glia and neurons as well as altering neurotransmitter systems [1]. Despite the widely reported neurotoxic effects of arsenic, cellular and molecular

mechanisms of arsenic toxicity on the central nervous system (CNS) have barely been studied.

Neurological toxicity	**Arsenic concentration** (urinary arsenic or water arsenic)	**Findings**	**Location**	**Reference**
Children cognitive deficits	10 and 50 µg/L	Dose–response relationships between arsenic concentration and children intellectual function	Bangladesh	Wasserman et al. 2004 [14]
The earliest manifestations of Alzheimer's disease	6.33 µg/L (a level below the current safety guideline of 10 µg/L)	Poorer neuropsychological functioning among community-dwelling adults and elders	Texas, U.S.	O'Bryant et al. 2011 [15]
Higher prevalence of psychiatric ailments	25 to µg/L	Increased risk of psychiatric disorder, depression, anxiety	West Bengal, India	Sen et al. 2012 [16]
Children intelligent development	Less than 50 µg/L	Lower verbal intelligence quotient (IQ) scores in Children	Mexico	Calderon et al., 2001[17]
Children cognitive dysfunction	Between 50 µg/L and 100 µg/L	Oppositional, Hyperactive and Attention-deficit/hyperactivity disorder (ADHD) -like behaviors in children	Mexico	Roy et al. 2011[18]
Higher risk of incident stroke	10 µg/L or less	More likely to report stroke	Michigan, U.S.	Lisabeth LD et al., 2010[19]

Table 1.1.2 Epidemiological evidence of arsenic effect on CNS

1.2 Brain endothelial cell

The BBB is a highly specialized structural and biochemical barrier that regulates the entry of blood-borne molecules into the brain and preserves ionic homeostasis within the brain microenvironment [20]. As the BBB plays an important role in CNS function, its dysfunction has been observed in various brain diseases including stroke, traumatic brain injury (TBI), neoplasia, multiple sclerosis, epilepsy, Alzheimer's disease, and vascular cognitive impairment [21].

Several animal studies have suggested that arsenic may cross the BBB and directly affect the CNS [1]. Arsenic may also have a toxic impact on the BBB itself and thus affect the function of CNS as it has been well documented that arsenic has a profound effect on the systemic vasculature. Recently, studies on the effects of mixed metals on the BBB showed that various metals, including arsenic, disrupted the integrity of the BBB likely via negative effects on astrocytes, leading to increased permeability of the BBB to toxicants and CNS neurotoxicity [22].

The BECs are the major component of BBB and form the major interface between the blood and the CNS [18]. The BECs have unique properties compared with endothelial cells in other tissues that allow them to tightly regulate the movement of ions, molecules, and cells between the blood and the brain. On one hand, BECs are held together by tight junctions (TJs) and adherent junctions (AJs). TJ components such as claudins, occludin, and junctional adhesion molecules interact with the actin cytoskeleton by scaffolding proteins such as zonula occludens-1 (ZO-1) forming a continuous belt-like structure, which restricts

paracellular permeability. AJ proteins, including VE-cadherin, mediate cell to cell contact that supports the barrier properties and regulates TJ expression in BECs [23]. On the other hand, BECs undergo extremely low rates of transcytosis as compared with peripheral endothelial cells, which greatly restricts the vesicle-mediated transcellular movement of solutes. Taken together, this tight paracellular and transcellular barrier creates distinct lumenal and ablumenal membrane compartments that tightly regulate molecular movement between the blood and the brain [24]. Since BECs play important roles in maintaining the functional integrity of brain tissue under toxic exposure, we used cerebral endothelial cells in our study to explore arsenic toxicity.

1.3 Arsenic-induced vascular dysfunction

Despite limited studies of arsenic's effects on BECs, its effects on endothelial cells from other tissues and organs have been reported. 'Blackfoot Disease' in Taiwan is one of the most interesting and unique clinical complications of human arsenic exposure. This disease is characterized by peripheral vasculature collapse followed by gangrenous tissue death of the extremities [25-27]. In addition, epidemiological studies have also indicated that incidences of cardiovascular diseases, including high blood pressure, arteriosclerosis, myocardial infarction, stroke and diabetes, were significantly increased in arsenic-exposed populations [28]. All these vascular injuries suggest a strong correlation between endothelial cell dysfunction and arsenic exposure. Therefore, our current study proposes that arsenic may have a direct effect on brain endothelial cells. Since increased vascular permeability (vascular leakage) is generally considered and used as a clinical and

pathological sign of early vascular injury, our study focused on arsenic's effects on brain endothelial cell permeability.

1.4 Oxidative Stress

1.4.1 ROS and RNS

Several studies of isolated vascular cells and tissues have provided clear evidence that arsenic stimulates the production of ROS and promotes oxidative stress in ECs [29]. Therefore, disruption of redox signaling is one of the potential mechanisms widely accepted in arsenic-induced toxicity in ECs [30, 31].

Oxidative stress results from an imbalance between the generation and detoxification of ROS. ROS is an umbrella term that generally refers to a family of oxidizing species derived from one- or two-electron reduction of molecular oxygen, including superoxide anion ($O_2^{\bullet -}$.), hydroxyl radical ($^{\bullet}OH$), and hydrogen peroxide (H_2O_2)[32]. Added to this list are other species such as peroxynitrite ($ONOO^-$) formed from $O_2^{\bullet -}$ and nitric oxide ($^{\bullet}NO$), nitrogen dioxide radical ($^{\bullet}NO_2$) formed from $ONOO^-$or myeloperoxidase (MPO)/ $H_2O_2^-$ dependent oxidation of nitrite anion (NO_2^-), which are also referred to as reactive nitrogen species (RNS) [33]. ROS are continuously generated by the mitochondrial electron-transport chain. In healthy cells, ROS levels are under homeostatic control by the endogenous antioxidant defense system that includes biological antioxidants such as glutathione (GSH), vitamin E, and vitamin C and antioxidant enzymes including catalase, superoxide dismutase (SOD), glutathione peroxidase (GPx), and heme-oxygenase I (HO-1). Thus, oxidative stress occurs when levels of ROS generated exceed the cellular antioxidant

capacity. In addition, RNS, include $^{\bullet}NO$, which is relatively unreactive, and its derivative, $ONOO^{-}$, which is a powerful oxidant, can act together with ROS to damage many biological molecules [34]. Therefore, these two species are often collectively referred to as ROS/RNS.

1.4.2 Oxidative Stress Affects BBB

Oxidative stress contributes to brain injury by reacting with proteins, lipids, and nucleic acids, as well as by activating a number of redox-sensitive signaling pathways [35] . Emerging evidence has shown that production of ROS can affect BBB permeability by a variety of mechanisms, including modulation of endothelial cell TJ and AJ proteins, such as ZO-1 and VE-cadherin [36].

BECs are equipped with a defense system against oxidative stress that includes increased levels of GSH, GPx(Glutathione peroxidase), SOD and catalase compared to the rest of the brain [37]. Among them, GSH in particular has been shown to play an important role in maintenance of BBB integrity. In addition, manganese-containing SOD (MnSOD/ SOD2) is found in the mitochondrial matrix while copper- and zinc-containing SOD (CuZnSOD) is found mostly in the cell cytosol. These enzymes aid in the conversion of $O_2^{\bullet-}$ to H_2O_2, which is also a ROS, but it is removed by catalase (and other enzymes) in BECs. In addition, $ONOO^{-}$, which can contribute to BBB breakdown, is also reduced through this conversion [38]. Without this system, $ONOO^{-}$ can rapidly form due to high concentrations of NO, particularly in the endothelial cells [39].

1.4.3 Mitochondrial Oxidative Stress

Mitochondria are considered one of the main sources of ROS production. It is estimated that approximately 0.2–2% of the oxygen taken up by a cell is converted by mitochondria to ROS, mainly through the production of $O_2^{\bullet-}$ [40]. The sites of $O_2^{\bullet-}$ production along the mitochondrial respiratory chain have been the subject of many studies. The two major sites of $O_2^{\bullet-}$ production are complex I (NADH–coenzyme Q reductase) and complex III (ubiquinone–cytochrome c oxidoreductase). Mitochondria produce superoxide anion predominantly from complex I when the matrix NADH/NAD^+ ratio is high. This leads to a reduced FMN site on complex I and reverse electron transport. In addition, complex III has also been regarded as a source of O^{2-} within mitochondria for a long time. When supplied with $CoQH_2$ and when the Qi site is inhibited by antimycin, complex III produces substantial amounts of $O_2^{\bullet-}$ from the reaction of O_2 with a ubisemiquinone bound to the Qo site [18]. However, ROS are also produced to a lesser extent outside of the mitochondrion [41].

1.4.4 ROS and Mitochondrial Dysfunction

Mitochondria are the most important target to study oxidative stress because they are not only the major source of ROS generation, but also sensitive targets of free oxygen radicals. Oxidative stress can induce mitochondrial DNA mutations, damage the mitochondrial respiratory chain, alter membrane permeability, influent Ca^{2+} homeostasis and affect mitochondrial defense systems [42].

As mentioned before, complexes I and III are thought to be major sites for the production of superoxide and other reactive oxygen species [41]. Thereby, free radical

attack occurs directly at these complexes in the mitochondrial respiratory chain. In addition, as mentioned above, the $O_2^{\bullet-}$ generated in mitochondria is converted to H_2O_2 by spontaneous dismutation or by SOD and converted to water by GPx or catalase. If this does not occur, H_2O_2 can undergo Fenton's reaction in the presence of divalent cations such as iron to produce $^{\bullet}OH$, which can be even more harmful to the mitochondrial biomolecules. The highly reactive $^{\bullet}OH$ can damage macromolecules within mitochondria, including lipids, proteins and DNA. The mitochondrial production of $O_2^{\bullet-}$ might be also modulated by NO, which can be converted to various reactive nitrogen species such as NO^- or the toxic $ONOO^-$ [43, 44].

Overall, ROS can damage mitochondrial NADH dehydrogenase, cytochrome c oxidase, and ATP synthase, leading to defective complex I and/or III function and further result in shutdown of mitochondrial energy production.

1.4.5 Oxidative Stress Measurement

Detection of Mitochondrial $O_2^{\bullet-}$ Using MitoSOX

In 2003, Kalyanaraman and colleagues created a superoxide-specific product from the reaction of DHE with $O_2^{\bullet-}$ [45]. Following this original report, DHE has been modified to allow detection of $O_2^{\bullet-}$ in the mitochondria by addition of a triphenylphosphonium group, which promotes its accumulation in the mitochondria. This modified DHE analog is referred to as MitoSOX and has become commonly used for detection of mitochondrial $O_2^{\bullet-}$. Briefly, MitoSOX reacts with mitochondrial $O_2^{\bullet-}$ to form 2-hydroxy-mito-ethidium (2-OH-Mito-E^+) (**Figure 1**), which is a fluorescent complex. Fluorescence measurements can

be made using the peak excitation wavelength of 510 nm with emission detection at 590 nm [46, 47]. In terms of its specificity for mitochondrial-derived $O_2^{\bullet-}$, previous studies have shown that blockade of mitochondrial complex 3 with antimycin A increases the conversion of MitoSOX to 2-OH-Mito-E but has no effect on conversion of DHE to 2-OH-E^+. In contrast, stimulation of cytoplasmic O^{2-} using phorbol-12-myristate-13-acetate (PMA) increases 2-OH-E^+ formation from DHE but does not increase formation 2-OH-Mito-E^+ from MitoSOX [48].

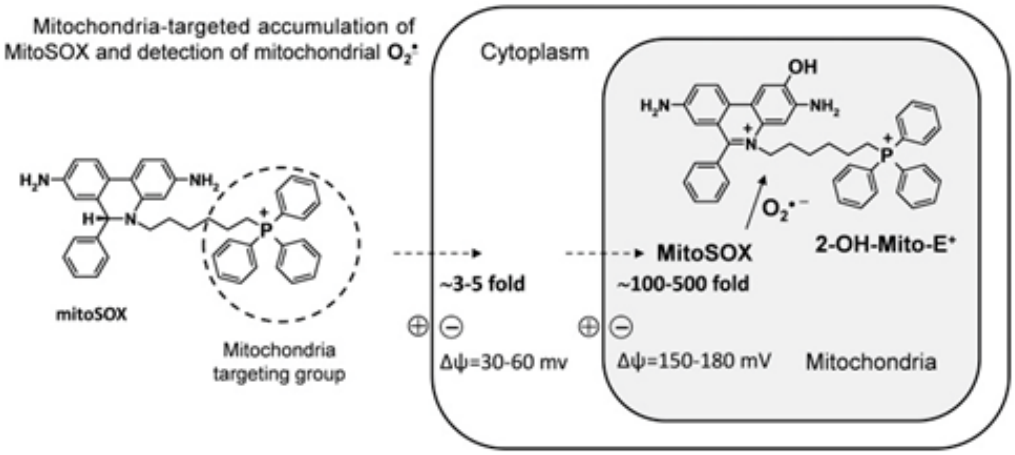

Figure 1.1 Mitochondrion-targeted accumulation of MitoSOX and detection of mitochondrial $O_2^{\bullet-}$[46]

ROS Detection Using EPR Spectroscopy

Direct detection of ROS and RNS is very difficult or impossible in solution at room temperature due to their very short half-life. Electron paramagnetic resonance (EPR) spectroscopy represents an alternative method for the detection of free radical formation.

EPR is a principally non-destructive, spectroscopic technique used to detect and identify paramagnetic species (species with unpaired electron(s)). The phenomenon of EPR is based on an intrinsic magnetic moment of the electron that arises from its spin. In most systems, electrons occur in pairs, such that the net magnetic moment is zero. However, if an unpaired electron is present, its magnetic moment can suitably interact with a magnetic field. The electron processes about the field axis with its magnetic moment either parallel or antiparallel to the field vector. This defines two energy levels [49].

As mentioned above, ROS half-life is too short compared to the EPR time scale so that they result in being EPR-invisible. However, they become EPR detectable once "trapped" and transformed in a more stable radical species. [46]. Among spin trapping or spin probe molecules, suitable for biological utilization, the CMH (1-hydroxy-3-methoxycarbonyl-2,2,5,5-tetramethylpyrrolidine) probe was adopted [50]. The superoxide free radical is known to react with the CMH probe, which is EPR silent, and converts it to a nitroxide radical (paramagnetic), which is EPR active and exhibits a characteristic triplet EPR signal. The specificity of CMH for superoxide free radicals has been well established. Thus, the appearance of a triplet EPR signal is indicative of superoxide and the peak height is a measure of the amount of superoxide accumulation in cultured cells and tissue samples [51](**Figure 2**).

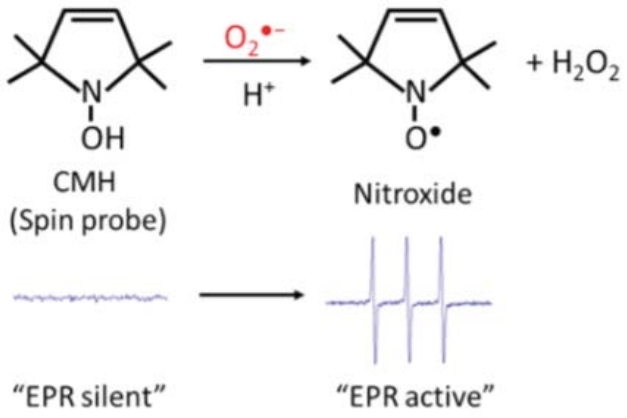

Figure 1.2 Spin probe CMH form stable adducts with radicals[52]

1.4.6 Antioxidant therapy

Even though antioxidant agents have not been used clinically to treat chronic arsenic poisoning, numerous experimental studies have shown the beneficial effects of antioxidant agents on in-vivo and in-vitro models exposed to arsenic treatment.

N-acetyl-cystine

N-acetyl-cystine (NAC) is an acetylated variant of the amino acid L-cysteine, which is able to increase cell protection to oxidative stress. NAC works as an effective scavenger of free radicals via interacting with ROS such as $^{\cdot}OH$ and H_2O_2. In addition, it predominately maintains the cellular GSH status and minimizes the oxidative effects of ROS through correcting or preventing GSH depletion [53]. Therefore, NAC has been used in the clinic to treat a variety of conditions including drug toxicity (acetaminophen toxicity) , human immunodeficiency virus/AIDS, cystic fibrosis (CF) , chronic obstructive pulmonary disease

(COPD) and diabetes. [54]. Interestingly, NAC was recently reported to reduce brain dysfunctions and neuropathies which further became a promising agent to treat vascular and nonvascular neurological disorders, via modulating glutamatergic, neurotrophic and inflammatory signaling pathways [55].

Tempol

Tempol (4-hydroxy-Tempo), is a redox-cycling (catalytic), metal-independent, and membrane-permeable antioxidant. It is a particularly attractive molecule because it promotes metabolism of $O_2^{\bullet -}$ at rates that are similar to SOD and is therefore considered a SOD mimetic. However, a recent report showed that tempol may facilitate metabolism of a wide range of ROS and RNS species, including OH^-, and exhibits catalase activity that further prevents generation of OH^- and H_2O_2 by Fenton reactions. Tempol also improves NO bioavailability and catalytically removes the highly reactive $ONOO^-$ species that is produced by the reaction between O_2^- and NO [56, 57]. Accordingly, Tempol has been studied in several models of oxidative stress. Tempol has been found to protect many organs, including the brain and the heart, from ischemia/reperfusion injury and improved survival in different models of shock. It also reduces brain or spinal cord damage after ischemia or trauma, among several other effects [58]. However, some studies have shown that tempol may have some toxic effects including impairing mitochondrial function in several cell lines [59, 60].

1.5 Autophagy

1.5.1 The Process of Autophagy

Autophagy is a catabolic process that degrades intracellular components through the lysosomal machinery. Three types of autophagy have been identified: 1) chaperone-mediated autophagy, which is a biochemical mechanism to deliver cytoplasmic proteins to lysosomes through the chaperone complex; 2) microautophagy, that directly uptakes cytoplasmic materials by lysosomes via a process similar to pinocytosis; and 3) macroautophagy, by which cytoplasmic organelles and proteins are delivered to lysosomes through the fusion of autophagosomes and lysosomes. Macroautophagy is the most studied type of autophagy and we focus on macroautophagy (here after referred to as autophagy) in our study [61].

The process of autophagy is initiated by the formation of a phagophore (or isolation membrane), which is likely derived from the lipid bilayer of the endoplasmic reticulum, Golgi apparatus, mitochondria or plasma membrane. The phagophore elongates and subsequently engulfs a portion of cytoplasm, thereby sequestering the cargo in a double membrane structure known as an autophagosome. The outer membrane of the autophagosome fuses with the lysosomal membrane to form an autolysosome, leading to the degradation of the autophagosomal inner membrane along with the sequestered materials by lysosomal acid proteases. The degradation products are then transported back into the cytoplasm to be recycled. Upon autophagy induction, the cytosolic LC3 (LC3-I) is conjugated to phosphatidylethanolamine (PE) to form lipidated LC3 (LC3-II). LC3-II binds to the expanding isolation membrane and remains bound to complete autophagosome. Therefore, LC3-II is widely used as a marker for autophagosomes [62] (**Figure 1.3**). One critical point is that autophagy is a multi-step process which includes not just the formation

of autophagosomes, but most importantly, flux through the entire system, including the degradation upon fusion with lysosomes. Assays that determine autophagic flux are crucial for the assessment of the dynamic autophagy process and help to distinguish between the accumulation of autophagosomes due to induced autophagic activity versus accumulation due to inefficient lysosomal clearance.

Currently, there is no single “gold standard” for determining autophagic activity that is applicable in every experimental context. There are four methods that are widely used to analyze autophagy, including LC3 turnover by immunoblotting, degradation of autophagic substrate p62 and tandem fluorescent-tagged LC3 assay to monitor autophagic flux. In addition, the fluorescence microscopy of LC3-positive vesicles is used to assess the static levels of autophagosomes. In most cases, it is highly recommended to combine multiple approaches to detect an autophagic response induced by a drug or treatment.

To date, the most experimentally straightforward method to monitor autophagic activity is the detection of LC3 protein processing. The amount of autophagosomes detected at any specific time point is a function of the balance between the rate of their generation and the rate of degradation though fusion with lysosomes [63]. Thus, we detected LC3-II formation by immunoblotting to monitor autophagic activity in our study. Furthermore, we used NH_4Cl, which can prevent lysosomal degradation of LC3-II by altering lysosomal pH to help us distinguish whether arsenic-induced-accumulation of autophagosomes are due to induced autophagic activity versus inefficient lysosomal clearance [64].

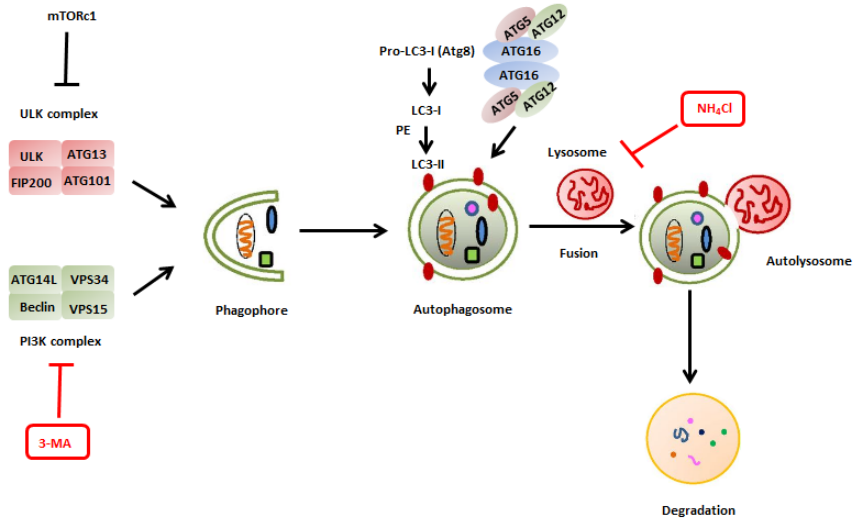

Figure 1.3 The process of autophagy. The autophagosome fuses with a lysosome to form an autolysosome, and then the cytoplasmic materials are degraded by the lysosome. The initiation step of autophagosome formation requires the ULK1-Atg13-FIP200 complex and Beclin1-class III PI3K complexes. Two conjugation systems, Atg12-Atg5-Atg16 and Atg8-PE, are essential for the elongation and enclosure step of the autophagosome formation. Lipid conjugation leads to the conversion of the soluble form of LC3-I to the autophagic vesicle-associated form LC3-II, which is commonly used as a marker of autophagy. mTOR plays a critical role in regulating autophagy**.** Figure adapted from Fig 1. in Ref[65]**.**

1.5.2 Autophagy Inhibitors

Since several studies have shown that autophagy is involved in many human diseases, various compounds or strategies have been utilized to induce or suppress autophagy both in vitro and in vivo.

Among them, 3-methyladenine (3-MA) is one of the most commonly used inhibitors in autophagy research today [66]. 3-MA inhibits autophagy by blocking autophagosome

formation via the inhibition of class III PI3K. In fact, PI3K plays an important role in many biological processes, including controlling the activation of mTOR, a key regulator of autophagy. In addition, many studies have revealed the protective effect of 3-MA. For instance, administration of 3-MA markedly reduced lung vascular leakage and tissue edema [67]. Moreover, 3-MA showed neuro-protective effects in seizure-induced brain injury [68]. Nevertheless, some nonspecific effects of 3-MA independent of autophagy inhibition have been reported, including inhibition of class I PI3K and mTOR, suppression of protein degradation, and cell migration and invasion [69].

1.5.3 Autophagy and Mitochondrial Oxidative Stress

It has been well known that the conditions which regulate the activity of the autophagic process are associated with cellular changes in the production of ROS/RNS. Not surprisingly, mitochondrial ROS production and oxidation of mitochondrial lipids have been shown to play a significant role in autophagy. It has been reported that rapamycin-induced autophagy in yeast is accompanied by the production mitochondrial superoxide and this effect can be inhibited by NAC [70]. In addition, starvation induced autophagy can be inhibited by overexpression of SOD2 and catalase, which reduced both $O_2^{\bullet-}$ and H_2O_2 levels [71].

In addition, autophagy also plays an important role in the regulation of mitochondrial function. It has been shown that mitochondria have an average half-life of 10–25 days in normal mammalian brains. However, during starvation, mitochondrial turnover can be accelerated by an autophagic process specifically called mitophagy [72]. In fact, damaged

mitochondria are typically programmed for removal by mitophagy and it has been shown previously that inhibition of mitophagy results in the accumulation of damaged mitochondria which further generate increased levels of reactive oxygen species.

Recent studies have demonstrated that arsenic can induce mitochondrial oxidative stress and the presence of ROS can trigger autophagy in other systems. However, the exact mechanism of how arsenic alters autophagy signaling is not fully investigated, especially in BECs.

1.5.4 Autophagy and Endothelial Permeability

Autophagy is active in endothelial cells in vitro and in vivo, but its functional role is quite controversial. In human umbilical vein endothelial cells (HUVECs), autophagy is induced upon silencing of vascular endothelial growth factor (VEGF), and subsequently leads to cell death [73]. Conversely, autophagy promotes cell survival in response to hypoxia in bovine aortic ECs (BAECs) cultured under glucose-deprived conditions [74]. More importantly, autophagy has also been implicated in regulating endothelial cell monolayer permeability. Some reports consider autophagy as a self-protective mechanism to maintain the endothelial cell permeability. Inhibiting autophagy in endothelial cells, either pharmacologically or by silencing ATG5 with siRNA, increases cellular ROS production which may impair ECs permeability. Therefore, some researchers suggest that ECs require autophagy to control ROS levels to maintain their permeability [4]. However, it has also been reported that loss of mitochondrial membrane potential under stress conditions is associated with an increase in autophagic activity [75]. Inhibition of autophagy

with a PI3K inhibitor (3-MA), or autophagosomal-lysosomal fusion inhibitors (bafilomycin A1 and chloroquine) can rescue some inflammatory factor (rMIF) induced vascular leakage [76]. To sum up, these studies support the notion that autophagy is a self-destructive mechanism instead of a cell survival mechanism.

1.6 Statement of Purpose

Arsenic is ranked first among toxicants that cause a significant potential threat to human health based on known or suspected toxicity [9]. Recently, arsenic-induced neurotoxicity has been widely reported. Several epidemiological studies have shown that even low concentrations of arsenic impairs neurological functions across a broad age range in human, leading to learning or memory deficits in childhood, impairing cognitive ability in adults and increasing the risk of neurodegenerative diseases or mood disorders [30, 77]. However, the cellular and molecular mechanisms of arsenic's effect on the CNS are not well understood. The BBB is a complex multicellular structure separating the CNS from the systemic circulation and its major functions include controlling molecular traffic, keeping out toxins, contributing to ion homeostasis and allowing immune responses, which suggest that disruption of the BBB is an important part in cellular damage in neurological diseases [78, 79] [80].

Therefore, we propose that arsenic may have a toxic impact on the BBB integrity and contribute to CNS dysfunction. Since BECs are the major units of the BBB, we focused on arsenic's effects on BECs in our study.

Previous studies have demonstrated that arsenic caused vascular dysfunction such as increased endothelial permeability and our laboratory has reported that ROS plays a significant role in arsenic-induced increase in brain endothelial cell permeability [3, 81, 82]. Mitochondria are considered as the major source of ROS generation in mammalian cells and it has been reported that mitochondria are a main target for arsenic toxicity [31]. Therefore, mitochondria may be the source of arsenic-induced ROS generation in ECs. In addition, autophagy, which is regulated by oxidative stress, plays an important role to control endothelial permeability and maintains redox balance in ECs and it may also be involved in arsenic toxicity in BECs [4]. Thus, we hypothesize that arsenic toxicity in BECs is mediated by mitochondrial oxidative stress and increased autophagyy. To test this hypothesis, we l studied the effect of sodium arsenite on RBE4 cells, which are commonly used to study BBB integrity and function.

To study the arsenic toxicity on mitochondrial oxidative stress in RBE4 cells, we determined the cell oxygen consumption and mitochondrial superoxide production in RBE4 cells after arsenite exposure for 24 hrs. Subsequently, we treated RBE4 cells with arsenite in the presence of antioxidant compounds to understand the relationship between arsenite induced mitochondrial oxidative stress and cellular dysfunction in RBE4 cells.

To identify the role of autophagy in arsenic-induced toxicity in RBE4 cells, we first detected autophagic activity under arsenite exposure using the autophagosome marker LC3II. Next, we further detected the autophagic activity in RBE4 cell under arsenic exposure with or without antioxidant to understand the relationship between arsenic-induced mitochondrial oxidative stress and autophagic activity. Finally, we treated the

RBE4 cells with arenite in the presence of autophagy inhibitors to investigate the role of arsenic-induced autophagy in increased permeability and mitochondrial dysfunction.

Taken together, we expect to reveal the potential mechanism of arsenic toxicity in brain endothelial cells, to understand the source of ROS production and the downstream pathway of ROS to induced brain endothelial dysfunction under arsenite exposure.

Chapter 2 Materials and Methods

2.1 Reagents

Name	Company	Catalog Number
Collagen I	Corning	354236
Sodium (meta)arsenite	Sigma-Aldrich	71287
N-Acetyl-L-cysteine	Alfa Aesar	A15409
4-Hydroxy-TEMPO	Sigma-Aldrich	176141
Fluorescein isothiocyanate–dextran	Sigma-Aldrich	FD40S
XF Assay Medium Modified DMEM	Seahorse Bioscience	102365-100
Oligomycin	Sigma-Aldrich	75351
Carbonylcyanide-4-(trifluoromethoxy)-phenylhydrazone (FCCP)	Sigma-Aldrich	C2920
Rotenone	Sigma-Aldrich	R8875
Antimycin A	Sigma-Aldrich	A8674
3-MA	EMD Millipore	189490

CMH. hydrochloride	Enzo Life Science	ALX-430-117-M010
Ammonium Chlorid	Fisher	A661-500
MitoSOX	Fisher	M36008

Table 2.1 List of major reagents used in this study

2.2 Methods

2.2.1 Cell Culture and Treatment

Rat brain endothelial (RBE4) cells, provided as a gift by Dr. Michael Aschner from the Albert Einstein College of Medicine, were grown until confluent on T25 flasks coated with rat tail collagen I at 50 μg/ml (354236, Corning). RBE4 (passage 1–20) were cultured in growth media composed of 44% alpha-MEM: 44% Ham's F-10 Nutrient (12571-063 and 11550-043, respectively; Invitrogen) supplemented with 10% heat-inactivated fetal bovine serum, plus freshly prepared 1 ng/ml basic fibroblast growth factor (PHG0264, Invitrogen), 300 μg/ml Geneticin (10131035, Invitrogen), penicillin/ streptomycin and maintained in a humidified 37 °C, 5% CO_2 incubator. Media was replaced every 2 days. 48 hours after plating, cells were treated with sodium arsenite at various concentrations.

1.3 mg of sodium arsenite was dissolved in 1 ml sterile water to prepare a stock solution of 10 mM and stored at -20°C up to 3 months. NAC was dissolved with PBS pH 7.4 to prepare as a stock solution of 100 mM and stored at 4°C. 3-MA (macroautophagy inhibitor) was prepared in culture medium and NH_4Cl (inhibitor of lysosomal function by increasing the intra-lysosomal pH) was dissolved in sterile water immediately before use.

2.2.2 Paracellular Permeability Assay

Paracellular permeability was detected as described previously [83]. Briefly, RBE4 cells were seeded at an initial density of 2×10^5 cells/cm^2 on the inner surface of polyethylene terephthalate (PET) cell culture inserts coated with 50 μg/ml of rat tail collagen I. The luminal and abluminal compartments were filled with 300 μl and 600 μl

RBE4 media, respectively. Cells were allowed to grow for 2 days at 37 °C in 5% CO_2 to confluency before arsenite treatment for 1, 3 or 6 days. Permeability of confluent monolayers was measured by adding FITC-labeled dextran (40kDa) to the upper chamber to a final concentration of 1 mg/mL. After incubation at 37°C, 5% CO_2 for 3 hrs, 50 µl of medium from the outside of the insert was taken and diluted to 500 µl with PBS. Fluorescence intensity of FITC-dextran was measured at the excitation wavelength of 492 nm and the emission wavelength of 520 nm by a fluorescent multi-mode microplate reader.

2.2.3 Mitochondrial Bioenergetics (mtBE) Assessment

RBE4 mtBE were analyzed using a Seahorse XF96 Analyzer. RBE4 cells were seeded in XF96-well plates (50,000 cells per well in 100 µl) and incubated overnight at 37°C, 5% CO_2 overnight. RBE4 media (80 µl) with sodium arsenite was added to achieve a final concentration of arsenite at 0, 2,5 and 10 µM (n=8 wells). After 24 hrs, cells were washed twice with pre-warmed XF assay medium containing 5 mM glucose, 1mM sodium pyruvate and incubated at 37°C without CO_2 at least 60 minutes prior to loading plate into the XF96 instrument. The sensor cartridge was loaded with oligomycin (20 µg/ml, port B), carbonyl cyanide 4-(trifluoromethoxy) phenylhydrazone (FCCP, 2µM, port C) and rotenone plus antimycin-A (1 µM each, port D) to measure the bioenergetic profile. Once the sensor cartridge was equilibrated, the calibration plate was replaced with the cell plate then introduced into the Seahorse Analyzer using a 3-minute mix cycle to oxygenate the medium followed by a 4 min measurement of the Oxygen Consumption Rate (OCR)

2.2.4 Superoxide Assessment by Electron Paramagnetic Resonance (EPR) Spectroscopy

An EPR instrument (Bruker BioSpin) was adopted for determining superoxide levels in RBE4 cells.

The EPR samples were prepared 24 hrs after arsenite treatment. RBE4 cells from 3 wells in 6-well plates were trypsinized and treated with 1 mM CMH for 3 hrs. The cells were washed with ice cold PBS and stored at -80 °C for further analysis [84].

Samples were assayed in 50 µL glass capillary tubes at room temperature using the Bruker e-scan EPR spectrometer. Spectrometer settings were as follows: sweep width, 100 G; microwave frequency, 9.75 GHz; modulation amplitude, 1 G; conversion time,5.12 ms; time constant 5.12 ms; receiver gain, 2×10^2; number of scans, 30 [85]. Quantification of the EPR signal intensity was determined by comparing the intensity of the recorded middle-derivative EPR peak of each sample.

2.2.5 Evaluation of Mitochondrial Oxidative Stress

RBE4 cells were seeded at a low density onto Lab-Tek eight-well chamber slides. After 24 hrs of arsenite exposure, mitochondrial ROS generation was determined using MitoSOX Redaccording to the manufacturer's instructions. Briefly, the cells were washed with PBS and incubated with fresh medium containing 2.5 µM MitoSOX for 20 min. The cells were loaded with 0.5 µg/mL Hoechst 33342 in HBSS for 5 min at 37 °C in the dark after washing 3 times with PBS. The excitation wavelength was 510 nm for MitoSOX and emission was measured at 580 nm. Images were taken using a Leica DMI4000 B microscope. Digital images from three wells were collected per experiment and corrected for autofluorescence, and background fluorescence was excluded from the calculations by

thresholding. The mean fluorescence intensity per image was calculated and averaged over the three images, using Image J software [86].

2.2.6 Immunoblotting

After treatments, total cell lysates were prepared with RIPA buffer. Protein concentrations were measured with the BCA Protein Assay according to the manufacturer's manual. Equal amounts (10-15 μg) of protein were separated by 12% sodium dodecyl sulfate-polyacrylamide gel electrophoresis and were transferred to polyvinylidene fluoride membranes. Membranes were incubated overnight at 4 °C with a 1:2000 dilution of anti-LC3B (ab43894) or 1:2000 dilution of anti-MnSOD (06984, Millipore). After additional incubation with a 1:3000 dilution of an anti-immunoglobin horseradish peroxidase-linked antibody (W4011, Promega) for 1 hour, the immune complexes were visualized using Supersignal™ chemiluminescent horseradish peroxidase substrate (32106, Thermo scientific). Densitometric analysis was performed using Image J analysis software (NIH). To normalize the protein levels, the intensity of band were first normalized to the mean intensity of the bands of control following by normalized to its beta-actin band.

2.2.7 Statistical Analysis

All data were pooled from at least three independent experiments. Student t-test was applied to determine the significance differences between two groups of samples. One-way ANOVA was used to determine overall significance differences followed by post hoc Tukey's test for multiple comparisons using SAS. All data are presented as mean ± SEM. Differences were considered statistically significant at $p < 0.05$.

Chapter 3 Results

3.1 Arsenite Induced Increased of Cell Monolayer permeability in RBE4 cells

The effect of arsenite on RBE4 cell monolayer permeability was assessed by FITC-dextran leakage assay. This method has been widely used to detect cell monolayer permeability in vitro. A confluent monolayer of RBE4 cells was grown on inserts was treated with 0-10 μM arsenite up to 6 days. The permeability of the monolayer was determined by measuring the content of FITC-dextran leaked from the insert to the medium of the plate well. For easy comparison, the percentage change of permeability was calculated from this basal value. As **Figure 3.1** shows, the cell monolayer permeability increased with arsenite concentration and exposure time. At the concentration of 5 μM, arsenite caused a significant increase in permeability after 6 days of treatment. However, cells treated with 10 μM arsenite had a significantly permeability increase at both day 3 and day 6.

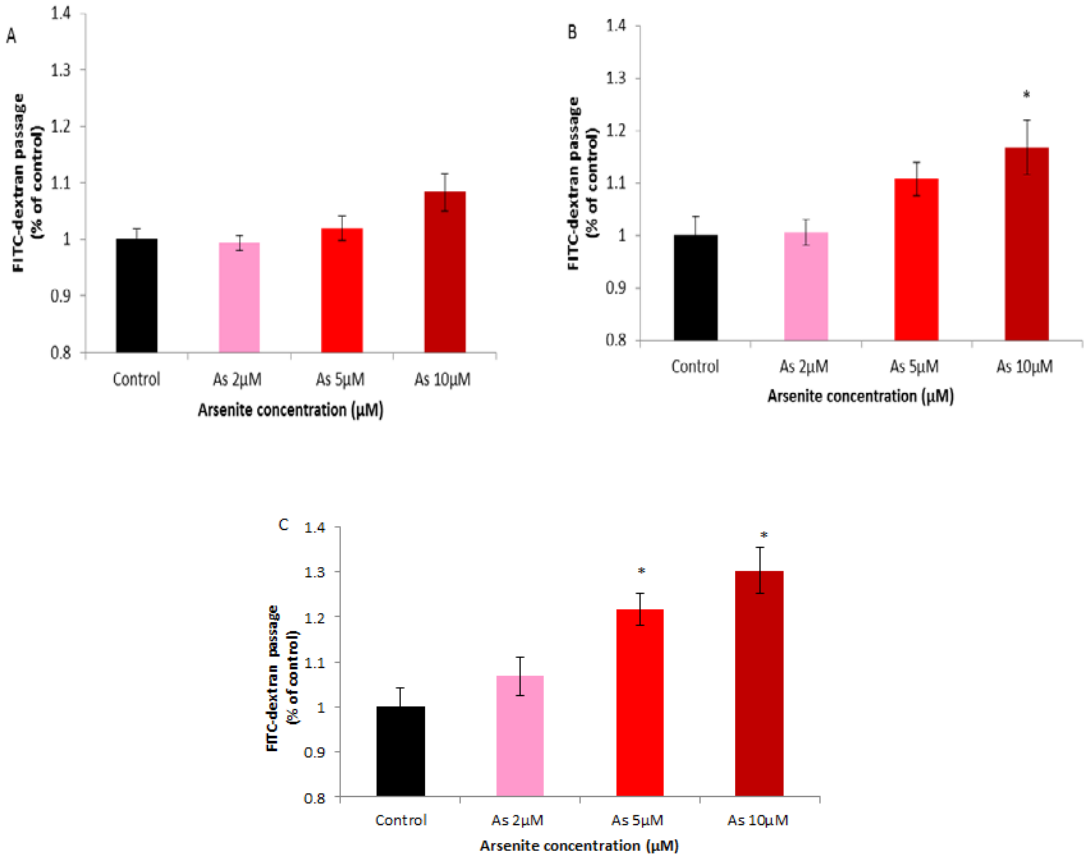

Figure 3.1 Arsenite increased RBE4 monolayer permeability. RBE4 cells in culture inserts were grown to monolayer and exposed to 0-10 μM arsenite for 1, 3, and 6 days. Fluorescence of FITC-dextran leaked from insert to plate well was assessed to determine the permeability. Data were normalized to the value of control (0 μM arsenite) of the same treatment day. A) RBE4 cells in culture inserts were grown to monolayer and exposed to 0-10 μM arsenite for 1 day. One-way ANOVA shows no significant main effect of 1 day As treatment on FITC dextran passage: $F(3, 32) = 2.84$, $P=0.053$ B) RBE4 cells in culture inserts were grown to monolayer and exposed to 0-10 μM arsenite for 3 days. One-way ANOVA shows significant main effect of 3 day As treatment on FITC dextran passage: $F(3, 32) = 4.29$, $P=0.011$. Post hoc by Tukey's multiple comparisons test shows FITC dextran passage was increased significantly in the group treated with 10 μM As compared to control group($*p<0.05$). C) RBE4 cells in culture inserts were grown to monolayer and exposed to 0-10 μM arsenite for 6 days. One-way ANOVA shows significant main effect of 6 day As

treatment on FITC dextran passage: $F(3, 32) = 8.92$, $P = 0.00019$. Post hoc by Tukey's multiple comparisons test shows FITC-dextran passage was increased significantly in the group treated with 5 μM and10 μM As compared to control group (*$p<0.05$). Results were presented as mean ± SEM. n=3.

3.2 Arsenite Increased ROS Production in RBE4 Cells

It is known that arsenic induces ROS generation in many types of endothelial cells [87]. To determine whether ROS is involved in arsenite-induced permeability in RBE4 cells, we evaluated the levels of ROS in RBE4 cells after 24 hrs of arsenite treatment (0-10 μM). Oxygen-derived free radical production from RBE4 cells was analyzed by EPR with the use of the spin probe, CMH. As noted in **Figure 3.2,** 5 and 10 μM arsenite treatment resulted in a significant increase in intensity of the EPR signal, indicating a significantly increased level of ROS production in RBE4 cells after arsenite treatment.

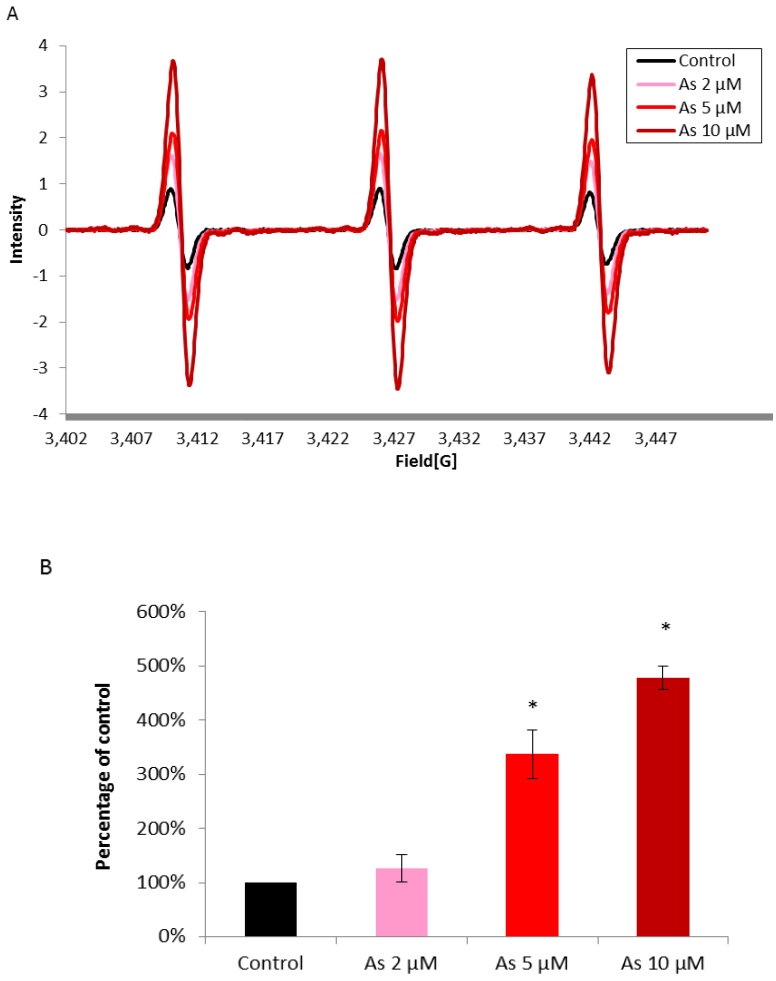

Figure 3.2 Arsenite Increased ROS Production in RBE4 Cells. A) EPR spectral profile of ROS production from RBE4 cells after 24 hrs various concentrations (0-10 µM) of sodium arsenite treatment. To detect levels of ROS, cell pellets were incubated with the spin probe CMH (1mM) for 3 hrs following a wash with iced cold PBS. B) Quantification of the EPR signal intensity was determined by comparing the intensity of the recorded middle-derivative EPR peak of each sample. Data were normalized to the value of control (0 µM arsenite) of each experiment; One-way ANOVA shows a significant main effect of As treatment on EPR intensity: $F(3, 8) = 9.72$, $P = 0.00013$. Post hoc by Tukey's multiple comparisons test shows that EPR intensity was increased significantly in the group treated with 5 µM As and 10 µM As compared to control group ($^*p<0.05$).). Results were presented as mean ± SEM. n=3.

3.3 Arsenite Induced RBE4 mtBE Loss in RBE4 Cells

Our present study provided evidence that arsenic induces oxidative stress in RBE4 cells. In addition, mitochondria are well known to play important roles in ROS generation and arsenic-induced mitochondrial dysfunction has been observed in many studies [31]. Based on these observations, we hypothesized that mitochondrial dysfunction following exposure to arsenic may be associated with the generation of ROS in RBE4 cells.

To assess this, we evaluated mitochondrial function in RBE4 cells in response to various concentrations of sodium arsenite. Mitochondrial function was evaluated by the Seahorse extracellular flux analyzer, which allows for real-time measurements of oxygen consumption and provides an overall assessment of cellular mtBE.

We found that arsenic has no effect on mitochondrial basal respiration and ATP-linked respiration in RBE4 cells. However, arsenic treatment decreased the oxygen consumption induced by FCCP, which is referred to as the maximal respiratory capacity (MRC), in a dose dependent manner in RBE4 cells (**Figure 3.3**). MRC reflects the rate of maximal electron transport and substrate oxidation achievable in the absence of limits imposed by the inner mitochondrial membrane proton gradient. Therefore, the decrease in MRC after arsenite treatment suggests that mitochondrial electron transport chains in the arsenite treated RBE4 cells were impaired.

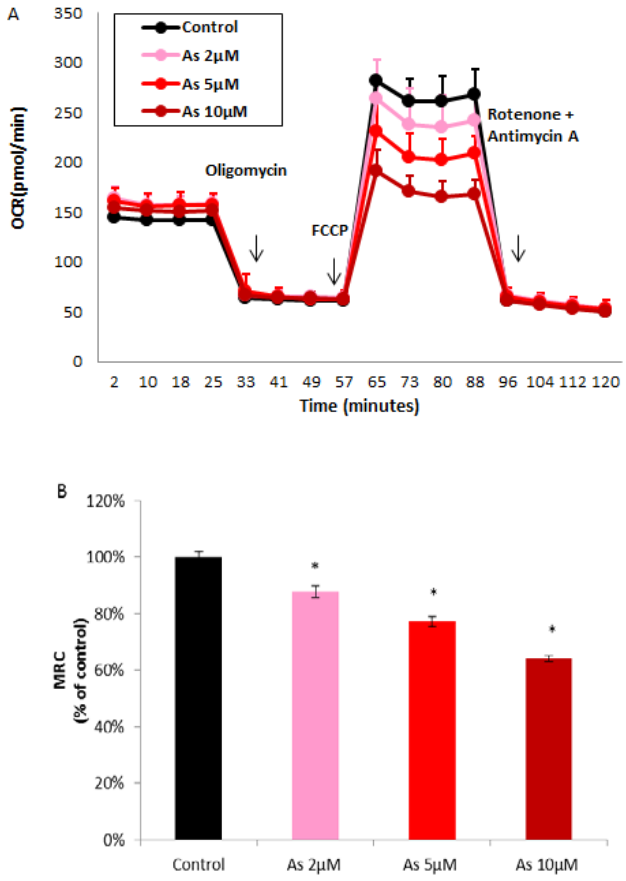

Figure 3.3 Arsenite decreased mtBE in RBE4 in a dose dependent manner. Oxygen consumption in RBE4 cells after 24 hrs exposure to sodium arsenite. OCR was manipulated with injections of oligomycin (20 µg/ml), FCCP (2 µM), and rotenone plus antimycin-A (1 µM). A) Representative bioenergetics profile of RBE4 cells treated with 2, 5, and 10 µM of sodium arsenite for 24 hrs. B) Quantification of MRC. MRC was achieved by adding 1 µM FCCP, a protonophore that dissipates the proton gradient across the inner mitochondrial membrane. Data were normalized by the value of control of each experiment. One-way ANOVA shows a significant main effect of As treatment on MRC: $F(3, 73) = 65.16$, $P < 0.0001$. Post hoc by Tukey's multiple comparisons test shows that MRC was increased significantly in the group treated with 2 µM As, 5 µM As and 10 µM As compared to control group (*$p<0.05$). Results were presented as mean ± SEM. n=6-8 per group from 3 independent experiments.

3.4 Arsenite Modulated Mitochondrial SOD in RBE4 cells

Manganese superoxide dismutase (MnSOD), also known as superoxide dismutase 2 (SOD2), is a primary mitochondrial antioxidant that neutralizes mitochondrial ROS through the conversion of superoxide to H_2O_2, and ultimately to H_2O by catalase [88].

As cellular antioxidant response appeared to directly correlate with mitochondrial dysfunction and mitochondrial oxidative stress, we next tested if 24 hrs of arsenite exposure in RBE4 cells changed MnSOD expression. Interestingly, we found that MnSOD expression significantly increased 35% after 2 µM arsenite exposure, while 5 µM and 10 µM arsenite increased MnSOD expression by 20% and 25% compared with vehicle treatment, respectively (**Figure 3.4**). Taken together, this result indicates that the effect of arsenite on MnSOD expression might be concentration-independent.

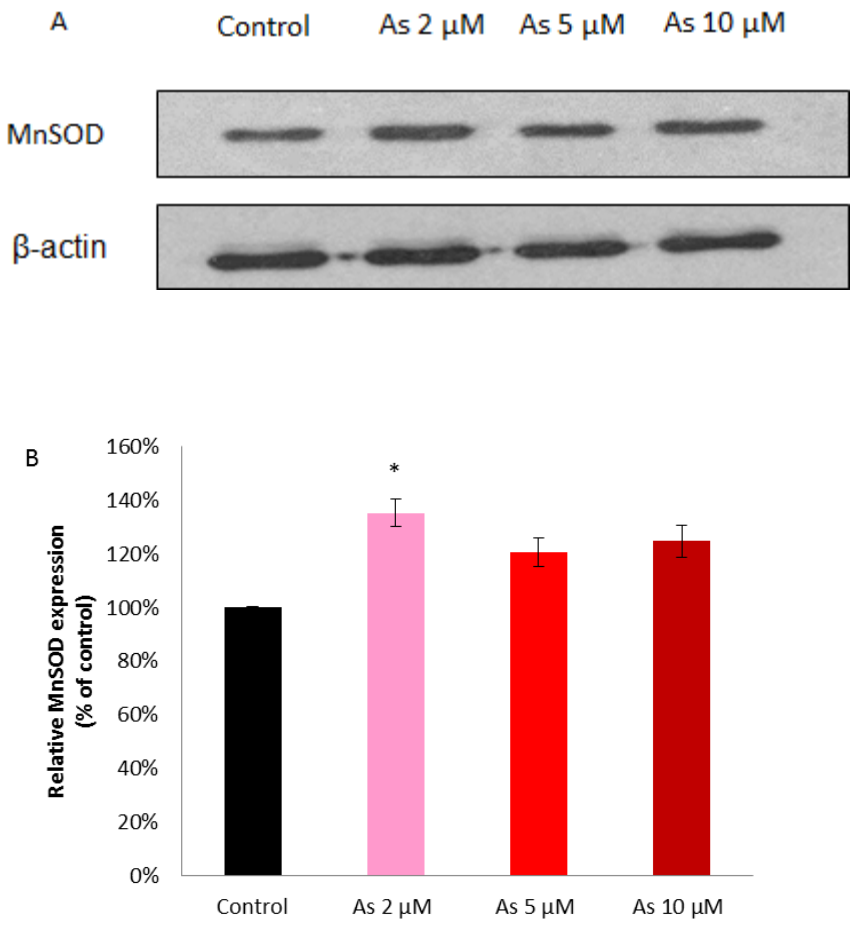

Figure 3.4 Arsenite affect MnSOD expression in RBE4 cells. RBE4 were treated with 0-10 µM arsenite for 24 hrs. Cell lysate was analyzed by immunoblotting for MnSOD formation. A) Changes in protein level of MnSOD. B) Densitometry analysis representing the relative MnSOD change in protein level in treated cells compared to controls. Data were normalized by the value of control. One-way ANOVA shows a significant main effect of As treatment on MnSOD expression: $F(2, 6) = 11.38$, $P=0.009$. Post hoc by Tukey's multiple comparisons test shows that MnSOD expression was increased significantly in the group treated with 2 µM As ($*p<0.05$). Results were presented as mean ± SEM. n=3.

3.5 Arsenite Induced Mitochondrial ROS Production in RBE4 Cells

As mentioned above, arsenite can induce cellular ROS generation. Results presented in **Figure 3.3 and Figure 3.4** suggested that arsenite exposure also resulted in mtBE loss and changes in mitochondrial antioxidant enzyme expression. To determine whether arsenite induces mitochondrial oxidative stress in RBE4 cells, we used live cell imaging of MitoSOX oxidation to detect ROS generation in mitochondria in our cell model. We found that 10 μM arsenite significantly promoted mitochondrial superoxide production in RBE4 cells (**Figure 3.5**). Overall, these results suggest that mitochondria play an important role in arsenite induced oxidative stress in RBE4 cells.

A

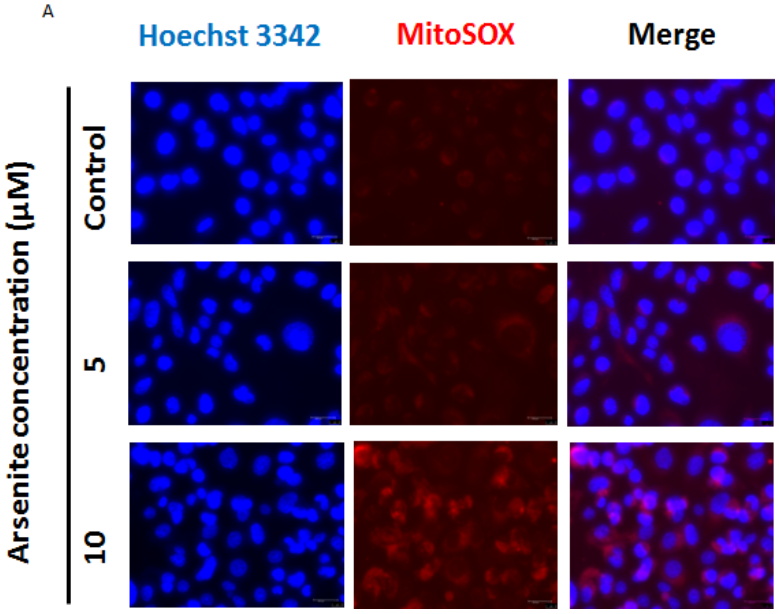
Hoechst 3342
MitoSOX
Merge
Arsenite concentration (µM)
Control
5
10

B

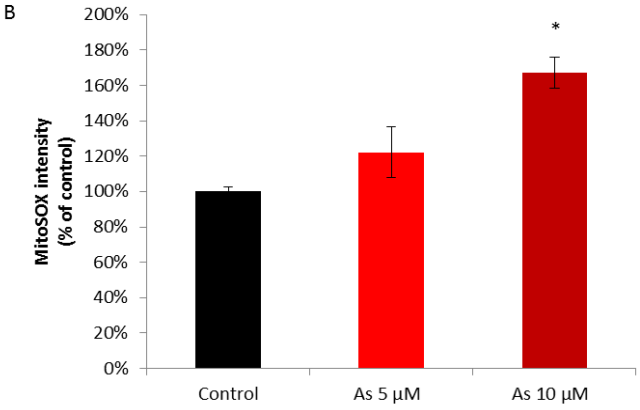
MitoSOX intensity (% of control)
200%
180%
160%
140%
120%
100%
80%
60%
40%
20%
0%
*
Control
As 5 µM
As 10 µM

Figure 3.5 Arsenite increased mitochondrial ROS production in a dose dependent manner in RBE4 cells. After treated with 5 or 10 μM of sodium arsenite for 24 hrs, RBE4 cells were incubated with MitoSOX and Hoechst 33342 to label mitochondrial superoxide radical (red) and nuclei (blue), respectively. A) Arsenite increased mitochondrial ROS production in a dose dependent manner. Scale bar, 20 μm; objective, 40X B) Quantification of MitoSOX staining intensity. The mean fluorescence intensity per image was calculated and averaged over the three images, using Image J software. Data were normalized by the value of control of each experiment. One-way ANOVA shows a significant main effect of As treatment on MitoSOX intensity: $F(2, 6) = 5.92$, $P=0.038$; Post hoc by Tukey's multiple comparisons test shows that MitoSOX intensity was increased significantly in the group treated with 10 μM As compared to control group (*$p<0.05$). Results were presented as mean ± SEM. n=3.

3.6 Antioxidant Decreased Arsenite-Induced Mitochondrial ROS Production

As shown in our previous experiments, arsenite exposure increased cellular ROS production as well as mitochondrial oxidative stress in RBE4 cells. Therefore, arsenic might induce toxicity in RBE4 cells via oxidative stress. To determine whether antioxidants rescue RBE4 cells from arsenic-induced mitochondrial oxidative stress, we treated RBE4 cells with 10 μM arsenite in the presence of the antioxidant NAC (2 mM) and superoxide anion radical scavenger tempol (500 μM). As **Figure 3.6** shows, NAC and tempol significantly inhibited arsenite induced-MitoSOX fluorescence in RBE4 cells.

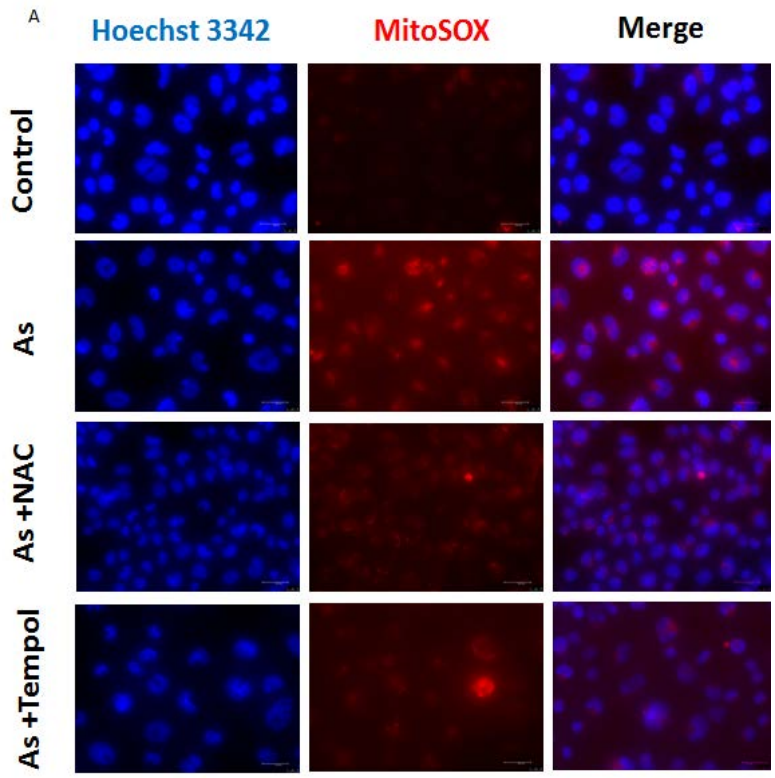
A
Hoechst 3342
MitoSOX
Merge
Control
As
As +NAC
As +Tempol

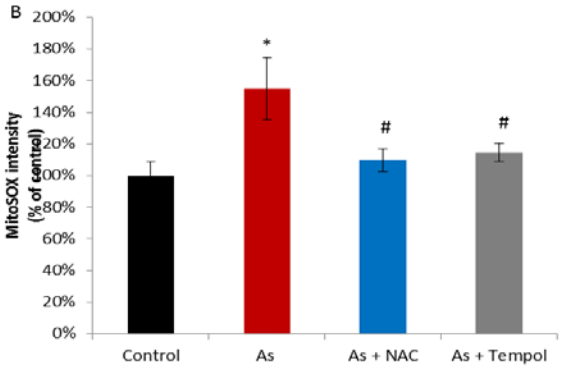
B
MitoSOX intensity (% of control)
200%
180%
160%
140%
120%
100%
80%
60%
40%
20%
0%
*
#
#
Control
As
As + NAC
As + Tempol

Figure 3.6 Antioxidant decreased Arsenite-induced mitochondrial ROS production. RBE4 cells were treated with 10 μM of sodium arsenite in the absence or the presence of NAC or tempol for 24 hrs. Cells were incubated with MitoSOX for 20 minutes and Hoechst 33342 to label mitochondrial superoxide radical (red) and nuclei (blue) respectively. A) Both NAC and tempol treatment decreased arsenite induced mitochondrial ROS production in RBE4 cells. B) Quantification of MitoSOX staining intensity. Data were normalized by the value of control of each experiment. Results are mean ± SEM. One-way ANOVA shows a significant main effect of different treatment on MitoSOX intensity: $F(3, 12) = 5.70$, $P=0.011$; Post hoc by Tukey's multiple comparisons test shows that MitoSOX intensity was increased significantly in the group treated with 10 μM As compared to control group (*$p<0.05$) and MitoSOX intensity was decreased significantly in the group treated with NAC and the group treated with tempol compared to As treatment group (# $p<0.05$). Results were presented as mean ± SEM. n=4.

3.7 Antioxidant Effects on Arsenite-Induced mtBE Loss in RBE4 Cells

Next, we investigated the effect of NAC and tempol on mitochondrial function under arsenic exposure. The cells were prepared for analysis of mtBE by Seahorse XF96 Analyzer as described in the Methods. As shown in **Figure 3.7**, NAC treatment can rescue the arsenic-induced decrease in mitochondrial maximal oxygen consumption, which suggests that that it can block arsenic induce mitochondrial ETC impairment in RBE4. Surprisingly, another antioxidant compound, tempol had no significant effect on arsenic-induced impairment of maximal mitochondrial respiration compared with arsenite treatment alone. Considering the different ROS targets of these two antioxidant compounds, besides superoxide, other oxidative stress species, such as NO derived from eNOS may also be involved in arsenite induced mitochondrial dysfunction in RBE4 cells.

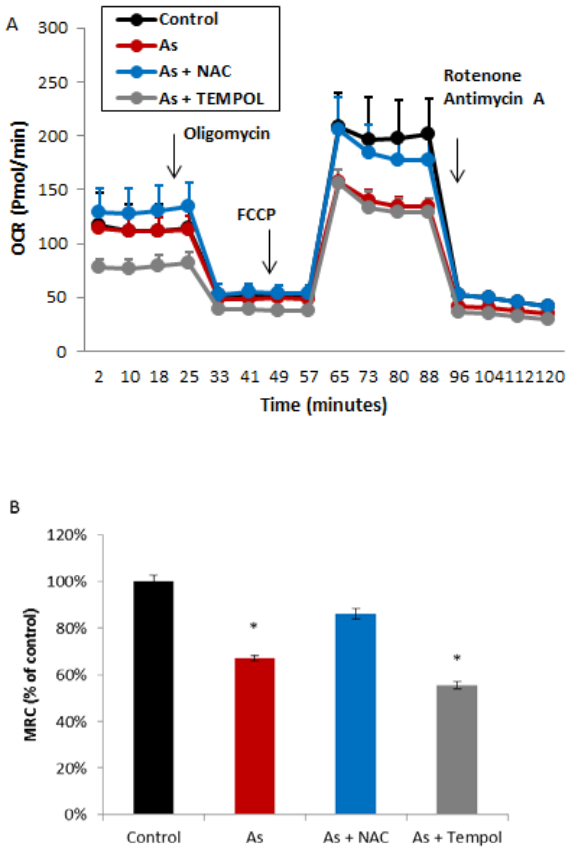

Figure 3.7 Antioxidant compound effects on arsenite-induced mtBE loss in RBE4 cells. Oxygen consumption of RBE4 cells after 24 hrs exposure to 10 µM sodium arsenite in the absence or presence of NAC or Tempol. OCR was manipulated with injections of oligomycin (20 µg/ml), FCCP (2 µM), and rotenone plus antimycin-A (1 µM). A) Represent bioenergetics profile of RBE4 cells treated with 10 µM arsenite and antioxidant compound. B) Maximal respiratory capacity (MRC) was achieved by adding 1 µM FCCP, a protonophore that dissipates the proton gradient across the inner mitochondrial membrane. Data were normalized by the value of control of each experiment. One-way ANOVA shows a significant main effect of different treatment on MRC: $F(3, 80) = 81.28$, $P<0.0001$. Post hoc by Tukey's multiple comparisons test shows that MRC was decreased significantly in the group treated with As and the group treated with As + Tempol compared to control group (*$p<0.05$). Results were presented as mean ± SEM. n=6-8 per group from 3 independent experiments.

3.8 Antioxidant Effects on Arsenite-Induced RBE4 Monolayer Permeability

Our previous findings have suggested that NAC can rescue arsenic-induced mitochondrial bioenergetics loss. Consistently, we found that NAC attenuated arsenite induced RBE4 monolayer permeability. In addition, another antioxidant compound tempol was unable to rescue arsenite induced RBE4 monolayer permeability (**Figure 3.8**), which is similar to our finding of its effect on mitochondrial function in RBE4 cells.

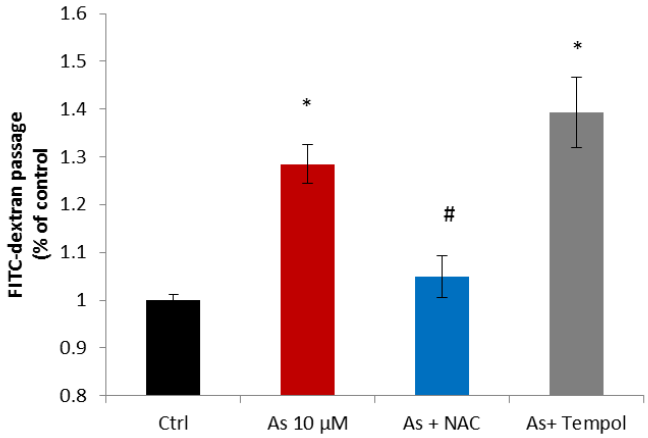

Figure 3.8 Antioxidant effects on arsenite-induced RBE4 monolayer permeability. RBE4 cells in culture inserts were grown to monolayer and exposed to arsenite (10 µM) with or without NAC (2 mM) or tempol (500 µM) for 6 days. The fluorescence of FITC-dextran leaked from insert to plate well was assessed to determine the permeability. Data were normalized by the value of control (0 µM arsenite) of same day. Results were presented as mean ± SEM. One-way ANOVA shows a significant main effect of different treatment on FITC-dextran passage: $F(3, 32) = 13.64$, $P= 0.00043$. Post hoc by Tukey's multiple comparisons test shows that FITC-dextran passage was increased significantly in the group treated with 10 µM As and treated with As + Tempol compared to control group ($*p<0.05$) and FITC-dextran passage was decreased significantly in the group treated with 10 µM As + NAC compared to As treatment group ($\# p<0.05$). n=3.

3.9 Arsenite Increased Autophagic Activity in RBE4 Cells

As mentioned in the introduction, autophagy is active in endothelial cells in vitro and in vivo. Recently, autophagy has been reported to be necessary for regulating endothelial function, either protectively or detrimentally [4, 89, 90]. Thus, it is interesting and important to explore whether autophagy may be involved in RBE4 function under arsenite exposure.

To explore whether arsenic alters autophagic activity in endothelial cells, we determined expression of autophagy markers in arsenic-treated RBE4 cells. Since the amount of LC3-II is clearly correlated with the number of autophagosomes, our approach was to detect LC3 conversion (LC3-I to LC3-II) in RBE4 by immunoblotting after 24 hrs treatment with various concentration of sodium arsenite. However, LC3-II itself is degraded by autophagy, making interpretation of the results of LC3 immunoblotting problematic. Since the amount of LC3 at a certain time point does not indicate autophagic flux, it is important to measure the amount of LC3-II delivered to lysosomes by comparing LC3-II levels in the presence and absence of lysosomal protease inhibitors. Therefore, in our experiment, a lysosomal inhibitor (20 mM NH_4Cl) was added 4 hrs prior to cell harvest to inhibit lysosome degradation. Another problem with this method is that LC3-II tends to be much more sensitive to be detected by immunoblotting than LC3-I. [91]. Accordingly, we compare the ratio of LC3-II to LC3-1 as well as the formation of LC3-II.

As shown in **Figure 3.9**, a significant increase of LC3-II was determined in RBE4 cells in the presence of lysosomal inhibitor NH_4Cl. In addition, both the formation of LC3-II and the calculated LC3-II/LC3-I ratio were increased significantly after arsenite exposure in the

absence and presence of NH_4Cl. Therefore, these data indicated that the increased LC3-II expression and LC3-II/LC3-I ratio is induced by the arsenite increased autophagic activity not due to compromised lysosome function.

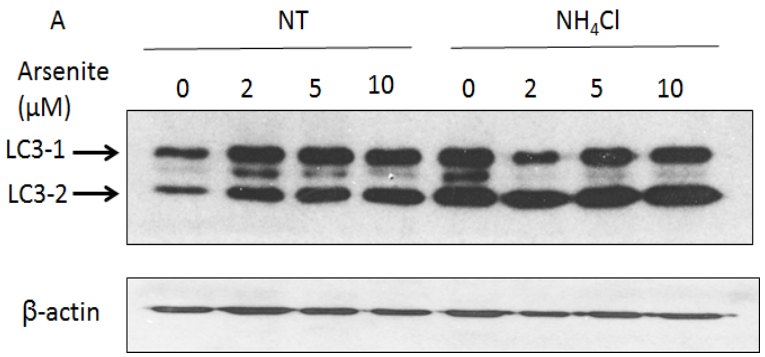
A
NT
NH4Cl
Arsenite (μM)
0 2 5 10 0 2 5 10
LC3-1
LC3-2
β-actin

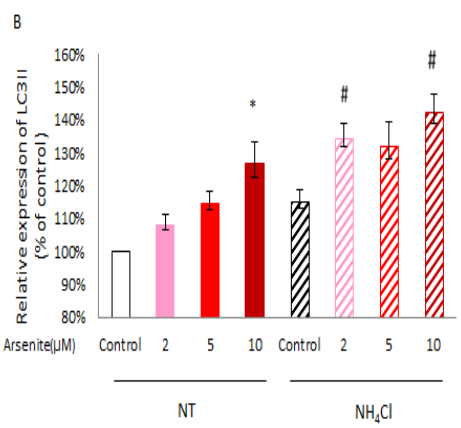
B
Relative expression of LC3II (% of control)
160%
150%
140%
130%
120%
110%
100%
90%
80%
Arsenite(μM) Control 2 5 10 Control 2 5 10
NT
NH4Cl

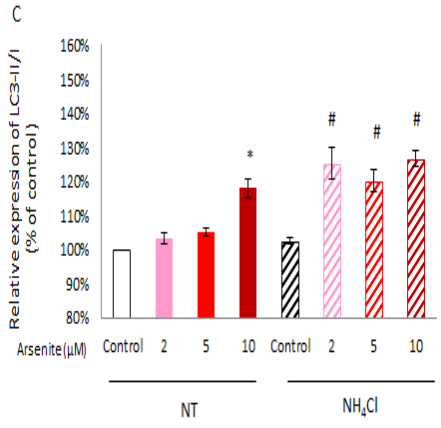
C
Relative expression of LC3-II/I (% of control)
160%
150%
140%
130%
120%
110%
100%
90%
80%
Arsenite(μM) Control 2 5 10 Control 2 5 10
NT
NH4Cl

Figure 3.9 Arsenite increased autophagic activity in RBE4 cells. RBE4 cells were exposed to 0-10 μM arsenite for 24 hrs. Lysosomal inhibitor (20 mM NH_4Cl) was added 4 hrs prior to cell harvest to inhibit lysosome degradation. Cell lysates were analyzed by immunoblotting for LC3-B formation. NT: no treatment

A) Immunoblotting of LC3-I and LC3-II.

B) Quantification LC3-II band density in arsenite treated cells compared to controls. Two-way ANOVA shows a significant main effect of As treatment on LC3-II: $F(3, 16) = 13.32$, $P<0.0001$. Two-way ANOVA also shows a significant main effect of NH4Cl treatment: $F(1, 16) = 24.61$, $P<0.0001$. Interaction between As treatment and NH4Cl treatment $F(3, 16) = 2.92$, $p=0.066$. Post hoc by Tukey's multiple comparisons test shows that LC3-II/I was increased significantly in the group treated with 10 μM As with NT compared to control with NT (*$p<0.05$) and in the 2 μM and 10 μM As treatment with NH_4Cl groups compared to control with NH_4Cl(#$p<0.05$).

C) Quantification LC3-II /LC3-I band density normalize to β-actin in arsenite treated cells compared to controls. Two-way ANOVA shows a significant main effect of As treatment on LC3-II/LC3-I: $F(3, 16) = 11.51$, $P=0.0003$. Two-way ANOVA also shows a significant main effect of NH_4Cl treatment: $F(1, 16) = 21.31$, $P=0.0002$. Interaction between As treatment and NH_4Cl treatment $F(3, 14) = 0.52$, $p=0.6685$. Post hoc by Tukey's multiple comparisons test shows that LC3-II/I was increased significantly in the group treated with 10 μM As with NT compared to control with NT group(*$p<0.05$) and in the 2μM, 5μM and 10 μM As treatment with NH_4Cl groups compared to control with NH_4Cl(#$p<0.05$).

Data were normalized by the value of control without NH_4Cl treatment. Results were presented as mean ± SEM; n=3.

3.10 Arsenite Increased Autophagic Activity in RBE4 cells by Oxidative Stress

Our previous results indicated that arsenic induced ROS generation in RBE4 cells. Further, many studies suggested that the presence of ROS can trigger autophagy in many systems [72]. To determine whether arsenite induced oxidative stress is involved in the increased autophagic activity, we treated RBE4 cells with 10 μM sodium arsenite in the presence of antioxidant NAC (2 mM) and tempol (500 μM). As shown in **Figure 3.10**, both NAC and tempol can efficiently block arsenite induced increased LC3-II expression as well as LC3-II/LC3-I ratio in the presence or absence of NH_4Cl, which suggest that arsenite increased autophagic activity in RBE4 cells was induced by ROS generation.

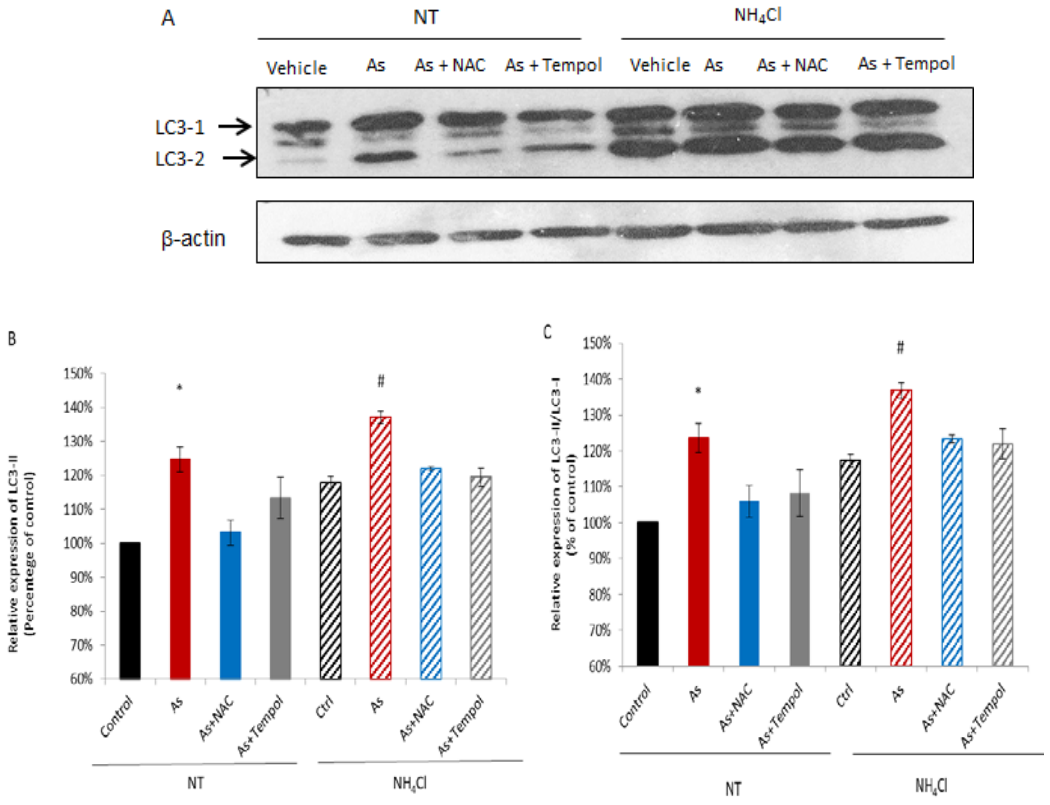
A
NT
NH4Cl
Vehicle
As
As + NAC
As + Tempol
Vehicle
As
As + NAC
As + Tempol
LC3-1
LC3-2
β-actin
B
Relative expression of LC3-II (Percentege of control)
150%
140%
130%
120%
110%
100%
90%
80%
70%
60%
*
#
Control
As
As+NAC
As+Tempol
Ctrl
As
As+NAC
As+Tempol
NT
NH4Cl
C
Relative expression of LC3-II/LC3-I (% of control)
150%
140%
130%
120%
110%
100%
90%
80%
70%
60%
*
#
Control
As
As+NAC
As+Tempol
Ctrl
As
As+NAC
As+Tempol
NT
NH4Cl

Figure 3.10 Arsenite increased autophagic activity in RBE4 cells by oxidative stress. A) RBE4 cells were treated with 10 μM arsenite in the presence of NAC (2 mM) and tempol (500 μM) for 24 hrs. Lysosomal inhibitor (20 mM NH_4Cl) was added 4 hrs prior to cell harvest to inhibit lysosome degradation. Cell lysate was analyzed by immunoblotting for LC3-B formation. NT: no treatment A) Immunoblotting of LC3-I and LC3-II.

B) Quantification LC3-II band density normalized to β-actom in arsenite treated cells compared to controls. Two-way ANOVA shows a significant main effect of As treatment on LC3-II: $F(3, 16) = 9.04$, $P=0.001$. Two-way ANOVA also shows a significant main effect of NH_4Cl treatment: $F(1, 16) = 20.80$, $P=0.0003$. Interaction between As treatment and NH_4Cl treatment $F(3, 16) = 1.05$, $P=0.398$. Post hoc by Tukey's multiple comparisons test shows that LC3-II was increased significantly in the group treated with 10 μM As with NT compared to control with NT group ($*p<0.05$) and in the 10 μM As with NH_4Cl treatment group compared to control with NH_4Cl treatment($\#p<0.05$).

C) Quantification LC3-II/LC3-I band density in arsenite treated cells compared to controls. Two-way ANOVA shows a significant main effect of As treatment on LC3-II/LC3-I: $F(3, 16) = 7.73$, $P=0.0021$. Two-way ANOVA also shows a significant main effect of NH_4Cl treatment: $F(1, 16) = 23.50$, $P=0.0002$. Interaction between As treatment and NH_4Cl treatment: $F(3, 16) = 0.24$, $P=0.867$. Post hoc by Tukey's multiple comparisons test shows that LC3-II was increased significantly in the group treated with 10 μM As with NT compared to control with NT group ($*p<0.05$) and in the 10 μM As with NH_4Cl treatment group compared to control with NH_4Cl treatment($\#p<0.05$).

Data were normalized by the value of control without NH_4Cl treatment. Results were presented as mean ± SEM. n=3.

3.11 3-MA Effects on Arsenite-Induced RBE4 Monolayer Permeability

To investigate whether the increased autophagic activity is involved in arsenite-induced increased RBE4 permeability, we used autophagy inhibition approach to test this hypothesis

3-MA is a commonly used autophagy inhibitor and it inhibits autophagy by blocking autophagosome formation via the inhibition of type III phosphatidylinositol 3-kinases (PI-3K). Therefore, we treated RBE4 cell with 10 μM arsenite in the absence or presence of 3-MA and then determined the RBE4 monolayer permeability using the paracellular permeability method.

First, we tested 3-MA (0-10 μM) effect on autophagic activity. As shown in **Figure 3.10 A** , 5 mM and 10 mM significantly decreased arsenite-induced LC3-II expression, In addition, 3-MA has been reported typically used at a concentration of 5 mM as an autophagy inhibitor [92]. Therefore, we use 3-MA at a concentration of 5 mM in our paracellular permeability study. Surprisingly, we found that 5 mM 3-MA treatment was unable to attenuate the arsenite-induced increased in monolayer permeability in RBE4 cells (**Figure 3.11 B**).

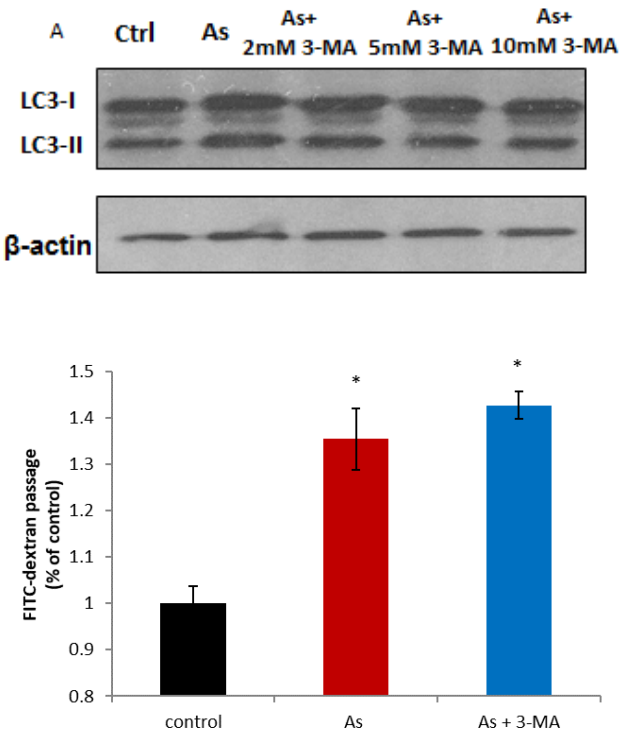

Figure 3.11 3-MA effects on arsenite-induced RBE4 monolayer permeability. A) RBE4 cells were exposure to 10 μM arsenite in the presence of autophagy inhibitor 3-MA (0-10 μM) for 24 hrs. Cell lysate was analyzed by immunoblotting for LC3-B formation. B) RBE4 cells in culture inserts were grown to monolayer and exposed to arsenite (10 μM) with or without 3-MA (5 mM) for 1,3, and 6 days. The fluorescence of FITC-dextran leaked from insert to plate well was assessed to determine the permeability. Data were normalized by the value of control (0 μM arsenite) of same day. One-way ANOVA shows a significant main effect of different treatment on FITC-dextran passage: $F(2, 24) = 20.82$, $P<0.0001$. Post hoc by Tukey's multiple comparisons test shows that FITC-dextran passage was increased significantly in the group treated with 10 μM As and treated with As + 3-MA compared to control group (*$p<0.05$). Results were presented as mean ± SEM. n=3.

3.12 3-MA effects on arsenite-increased Mitochondrial SOD expression

To investigate the effect of autophagy inhibitors on the mitochondria antioxidant system, we determined the effects of 3-MA on arsenite increased MnSOD expression in RBE4 cells.

Our previous results suggested that 2 μM arsenite significantly increased MnSOD expression in RBE4 cells. Therefore, we treated RBE4 cells with 2 μM arsenite in the presence of 5 mM 3-MA to study autophagy inhibitor effects on MnSOD expression. We found that 3-MA treatment further increased arsenite-induced MnSOD overexpression in RBE4 cells (**Figure 3.11**).

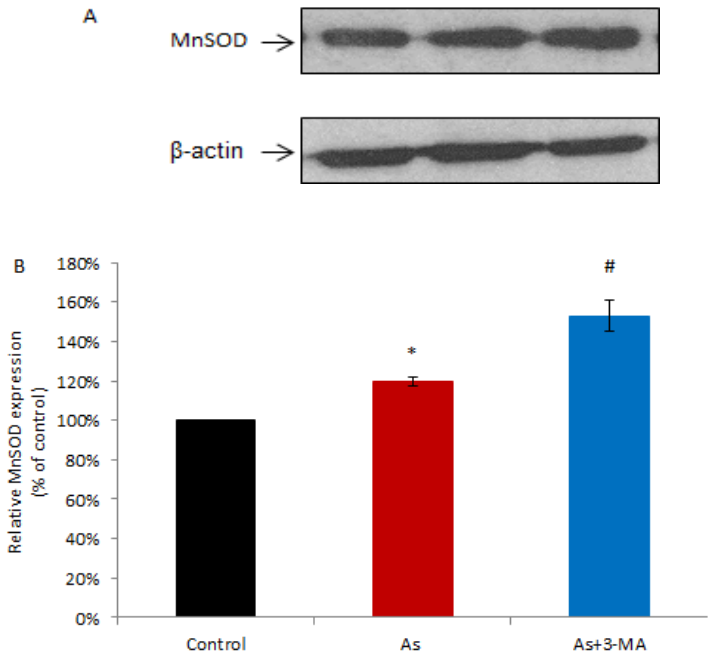

Figure 3.12 3-MA effects on arsenite-increased Mitochondrial SOD expression. RBE4 cells were treated with 10 μM arsenite in the absence of presence of 5 mM 3-MA for 24 hrs. Cell lysate was analyzed by immunoblotting for MnSOD formation. A) Changes in protein level of MnSOD. B) Densitometry analysis representing the relative change in protein level in treated cells compared to controls. Data were normalized by the value of control. One-way ANOVA shows a significant main effect of As treatment on MnSOD expression: $F(2, 6) = 20.18$, $P=0.002$. Post hoc by Tukey's multiple comparisons test shows that MnSOD expression was increased significantly in the group treated with 2 μM As compared with control($*p<0.05$) and in the group treated with As + 3-MA compared with treated with 2 μM As ($\#p<0.05$). Results were presented as mean ± SEM. n=3

3.13 3-MA effects on arsentie-induced mtBE loss in RBE4 cells

To determine whether 3-MA has effects on arsenite- induced mtBE loss in RBE4 cells, we treated RBE4 cells with 10 μM arsenite in the absence or presence of 5 μM 3-MA. The cells were then prepared for analysis of mtBE by Seahorse XF96 Analyzer as described in the Methods. Considering 3-MA may have effects on RBE4 cell viability, we further normalized RBE4 cells oxygen consumption by protein concentration using BCA assay.

As shown in **Figure 3.12**, we found that 5mM 3-MA significantly increased the MRC of RBE4 under normal condition. However, 5 mM 3-MA had no effect on the MRC of RBE4 cells under arsenic exposure.

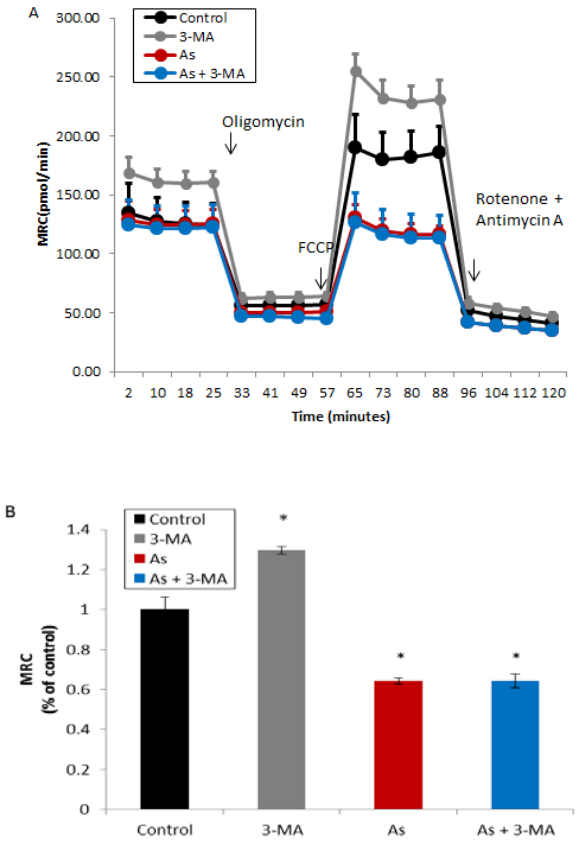

Figure 3.13 3-MA effects on arsenite-induced mtBE loss in RBE4 cells. Oxygen consumption of RBE4 cells were determined after 24 hrs exposure of 10 µM sodium arsenite in the absence or presence of 5 mM 3-MA. OCR was manipulated with injections of oligomycin (20 µg/ml), FCCP (2 µM), and rotenone plus antimycin-A (1 µM). A) Represent bioenergetics profile of RBE4 cells treated with arsenite and antioxidant compound. B) Quantification of MRC. Data were normalized by the value of control of each experiment. One-way ANOVA shows a significant main effect of different treatment on MRC: $F(3, 24) = 55.38$, $P<0.0001$. Post hoc by Tukey's multiple comparisons test shows that MRC was increased significantly in the group treated with 3-MA compared to control group and was decreased significantly in the group treated with As and As + 3-MA compared to the control group (*$p<0.05$). Results were presented as mean ± SEM. n=6-8 per group from 3 independent experiment

Chapter 4 Discussion

Arsenic is a major health concern globally, with over 100 million people exposed to unhealthy levels of inorganic arsenic through contaminated drinking water. Recently, arsenic exposure was reported to cause CNS alterations, including learning, memory, and concentration deficits [93]. Despite these widely reported neurotoxic effects, the cellular and molecular mechanisms of arsenic on the CNS are not well understood. As brain endothelial cells play important roles in maintaining the functional integrity of brain tissue under toxic exposure, we focused on alterations in cerebral endothelial cells after arsenic treatment to study the mechanism of arsenic toxicity in our study.

Vascular permeability is considered as an important indicator of BECs function. In fact, it is regulated, in part, through changes in paracellular permeability which refers to the movement of substances across the endothelial barrier via the intercellular space between adjacent endothelial cells [94]. Therefore, we focused on arsenite's effects on RBE4 paracellular permeability to study arsenic toxicity in endothelial cells in our experiments.

Using a 40-kDa molecular weight tracer, we found a dose and time dependent increase in FITC-dextran permeability RBE4cells. . This result indicates that arsenite treatment increased paracellular permeability in RBE4 cells. More importantly, our findings from RBE4 cells are consistent with what we observed previously with b.End3 cells. Similar to the results in RBE4, we found arsenite increased paracellular permeability and we further reported non-uniform disruption of VE-cadherin or ZO-1 and increased gap formation between adjacent cells in b.End3 model [3].

In our experiments, we studied arsenic toxicity using an in vitro model of BBB consisting of brain endothelial cells. However, it should be acknowledged that the BBB is formed of several cell types, such as endothelial cells, astrocytes, perivascular microglia, pericytes and neurons, and their interactions determine the BBB function [95]. Therefore, we should note that the results presented in our current study have some limitations. However, it provides proof of principle that arsenic toxicity may increase BBB permeability in the on CNS and supports for future studies with animal models.

Studying the mechanisms of toxicity by inorganic arsenic species is a complex task, as arsenic interacts with a large number of targets to disrupt a large number of cellular processes. Among them, ROS have been reported to play an important role in arsenic toxicity both in carcinogenic or non-carcinogenic studies [96, 97]. Therefore, further studies of the sources of ROS and how they are produced is a worthwhile effort in investigating mechanisms of arsenic toxicity. Previously, our laboratory has reported that NADPH oxidase may not be an important player in arsenite-induced ROS production in brain endothelial cells. We found arsenic did not significantly increase NADPH oxidase activity in bEnd3 until its concentration reached 20 μM and the NADPH oxidase inhibitor, DPI did not rescue changes in barrier function of bEnd3 cells that were exposed to 10 μM arsenite for 6 days [3]. Besides NADPH oxidase, mitochondria are also well recognized as main sources of arsenic-induced ROS generation and impaired mitochondrial function has been found upon arsenic exposure in many in vitro and in vivo models [31, 98]. Accordingly, we determined whether mitochondria are involved in ROS generation under arsenic exposure in RBE4 cells.

Our current study further confirmed arsenic induced ROS production in BECs using CMH spin trap with EPR spectroscopy. We found an increasing free radical signal in RBE4 cells with increased arsenic concentration, which indicated that arsenic-induced ROS generation occurs in a concentration dependent manner. More importantly, we found that sodium arsenite dose-dependently increased mitochondrial superoxide and altered MnSOD expression in RBE4 cells. In addition, arsenic exposure also resulted in decreased mtBE in RBE4 cells. Therefore, we concluded that mitochondria were important targets for the arsenic toxicity and arsenic may induce oxidative stress via mitochondrial ROS generation in BECs.

To further confirm the role of oxidative stress in arsenic toxicity in BECs, we treated RBE4 cells in the presence of two antioxidant compounds: NAC and tempol. We found that both NAC and tempol rescued arsenite-induce mitochondrial superoxide production as determined by MitoSOX staining. In addition, NAC also rescued the arsenic-induced decreased mtBE and increased monolayer permeability in RBE4 cells. However, another antioxidant tempol had no significant effect on arsenic-decreased in mtBE and increased permeability in RBE4 cells. Taken together, these data suggest that arsenite-induced ROS in RBE4 cells is mainly generated from mitochondria, and the increased ROS causes further damage to mitochondria to inhibit their function. In turn, these malfunctioning mitochondria can produce more ROS leading to sustained ROS accumulation. The arsenic-increased ROS generation is responsible for increased monolayer permeability in RBE4 cells.

In our experiments, we identified mitochondrial ROS generation as an important source of arsenic-induced oxidative stress in BECs. However, arsenite may also generate

ROS production outside mitochondria, especially since tempol could not block arsenic-induced permeability in RBE4 cells, which suggests $O_2^{\bullet-}$ is not the only ROS species induced by arsenic. Our previous result has suggested that NADPH oxidase may not be involved in arsenic-induced oxidative stress in BECs [78]. Besides NADPH oxidase and mitochondria, other sources of ROS production that are induced by arsenic have been recognized. It has been suggested that arsenic may induce oxidative stress by cycling oxidative states such as Fe, or by interacting with antioxidant and increasing inflammation, resulting in the accumulation of ROS in cells. Therefore, more research needs to be done to investigate the source of ROS in BECs under arsenic exposure.

Another important finding of our study is that the general antioxidant NAC rescued arsenic-induced toxicity including the decreased mtBE as well as the increased endothelial cell permeability in RBE4 cells; we did not observe this effect with the superoxide scavenger tempol. It is generally assumed that the action of NAC results from its antioxidative or free radical scavenging property as an antioxidant through increasing intracellular GSH levels [99]. In contrast, tempol mainly promotes metabolism of $O_2^{\bullet-}$ at rates that are similar to SOD. Therefore, we propose that arsenite induced-toxicity in RBE4 may not occur only via generation $O_2^{\bullet-}$, but also through other oxidative stress species as well, such as H_2O_2. In addition, another possible explanation is that tempol may have toxic effects in RBE4 cells. As mentioned in the Background, tempol is a cell membrane-permeable amphilite nitroxide and improves NO bioavailability in vitro and in vivo. NO inhibits the mitochondrial cytochrome c oxidase (complex IV) in competition with oxygen [100]. Additionally, tempol has been reported to have toxic effect in many cell models. To

further confirm whether NAC can be a therapeutic approach for arsenic-induced toxicity in BECs, more in vivo studies need to be done.

An interesting link between ROS production and arsenic toxicity in endothelial cells might be autophagy. Autophagy is a highly conserved process in eukaryotes in which the cytoplasm, including excess or aberrant organelles, is sequestered into double-membrane vesicles and delivered to the degradative organelle, the lysosome/vacuole, for breakdown and eventual recycling. This process has an important role in various biological events such as adaptation to changing environmental conditions, cellular remodeling during development and differentiation, and determination of lifespan [101]. Although autophagy may also mediate protective effects against some diseases, many studies have shown that autophagy is involved in many pathological conditions. In recent years, research on the autophagy has greatly increased. An advanced understanding of the importance of autophagy in vascular physiology led us to investigate the correlation of autophagy with endothelial barrier dysfunction [102]. Autophagy induction has been reported to increase angiogenesis in BAECs [103]. In addition, Western blot results have shown that the mTOR inhibitor rapamycin induced autophagy, which is indicated by the increased level of autophagy markers LC3 and beclin-1, [104]. Meanwhile, autophagy has been reported to mediate the degradation of the junction protein ZO-1 and VE-cadherin in HMEC-1 cells, resulting in an increase in vascular permeability [76]. Therefore, we determined whether autophagy is involved in arsenic toxicity in RBE4 cells.

In our present experiment, 24 hrs arsenic treatment increased the expression of LC3-II and the LC3-II/ LC3-I ratio in the presence and absence of a lysosome inhibitor NH_4Cl.

These results demonstrated that the increased level of autophagy markers in RBE4 cells is due to arsenic increased autophagic activity not a compromised lysosome activity. In addition, we found both NAC and tempol rescued arsenic-induced increased expression of LC3-II as well as LC3-II/LC3-I ratio in RBE4 cells. Taken together, our study indicated arsenic-induced autophagy by ROS generation in RBE4 cells.

To investigate the role of autophagy in arsenic toxicity in RBE4, we treated RBE4 cells with arsenite in the presence of 3-MA, which has been widely used as an autophagy inhibitor based on its inhibitory effect on class III PI3K activity. We found that 3-MA reduced the increase in LC3-II and LC3-II/LC3-I ratio in RBE4 cells induced by arsenate treatment. However, 3-MA didn't rescue the arsenic-induced increase in permeability. In addition, although 3-MA further increased the MRC in RBE4 under control condition, it did not rescue the arsenic-induced decline in mtBE. One of the important problems using 3-MA is that it may have dual roles in modulating autophagy via different temporal patterns via inhibition of class I and III phosphoinositide 3-kinases. Recently, an increased level of autophagy has been found in cells treated with 3-MA for a prolonged period [66]. In our experiment, we only confirmed that 3-MA reduced arsenic-induced autophagy after 24 hrs treatment. However, we treated RBE4 cells with 3-MA and arsenite for 6 days to perform paracellular permeability assays in RBE4 cells. Since the major limitation of the RBE4 models is the relatively high paracellular permeability to small molecules, the RBE4 model may be unable to show us the effect of autophagy inhibitor on arsenic-induced permeability.

Therefore, more experimental approaches and more autophagy inhibitors should be used to study the role of autophagy in arsenic toxicity in BECs. As mentioned above, we

investigated the effect of 3-MA on BECs permeability by using paracellular permeability assay in RBE4 cells, which is limited to studying the endothelial permeability of small molecules. Thus, it will be worthwhile to study if 3-MA has effects on RBE4 TJs and AJs protein such as ZO-1 and VE-cadherin. In addition, during the study of autophagy mechanisms, other autophagy inhibitors besides 3-MA have been used in many studies. For example, Lys 05, which accumulates within and deacidifies the lysosome, resulted in impaired autophagy and tumor growth in many studies [105]. Interestingly, as a new lysosomal autophagy inhibitor, Lys05 has a better therapeutic index and has the potential advantage to be developed further into a drug for autophagy-targeting therapy [106].

In addition, the relationship between autophagy and vascular permeability factors is also worthwhile to study. Vascular endothelial growth factor (VEGF) is a key regulator of vascular permeability [107]. Detailed analysis of the published literature has shown that in vivo and in vitro VEGF-mediated permeability has common involvement of many specific signaling pathways, in particular of junctional signaling proteins such as vascular endothelial cadherin and the tight junctional proteins zona occludens and occludin linked to the actin cytoskeleton [108]. Research in our laboratory previously reported VEGF antibody reversed VE-cadherin and ZO-1 disruption induced by arsenite, which suggests that up-regulated VEGF may play an important role in the arsenite-induced permeability increases in ECs [3]. Recently, the relationship between the role of VEGF and autophagy has been reported [109]. Autophagy was reported to drive the secretion of VEGF in mesenchymal stem cells (MSC) [110]. In addition, inhibiting autophagy could impair VEGF-induced angiogenesis in cultured bovine aortic endothelial cells (BAECs) [111].Therefore, it is very

important to study the relationship between autophagy and VEGF overexpression in arsenic treated ECs.

In summary, our present results provide a potential mechanism by which arsenic induces toxicity in brain endothelial cells (**Figure 4.1**). We have identified that arsenic-induced mitochondrial dysfunction might be an important source of ROS generation, and the increased ROS may cause further damage to mitochondria and inhibit their function. In turn, these malfunctioning mitochondria can produce more ROS causing a loop of increasing ROS. We also found that arsenic-increased ROS generation plays an important role in arsenic-induced endothelial permeability in BECs by using antioxidant treatment. We have further identified NAC was an efficient treatment for arsenic-induced increased permeability and mtBE loss in RBE4 cells. In addition, we also found that arsenic-induced autophagy via ROS generation and it may be involved in arsenic toxicity in endothelial cells. However, the role of autophagy in BECs permeability is still unclear and more research needs to be done to determine its function in arsenic-induced toxicity in endothelial cells.

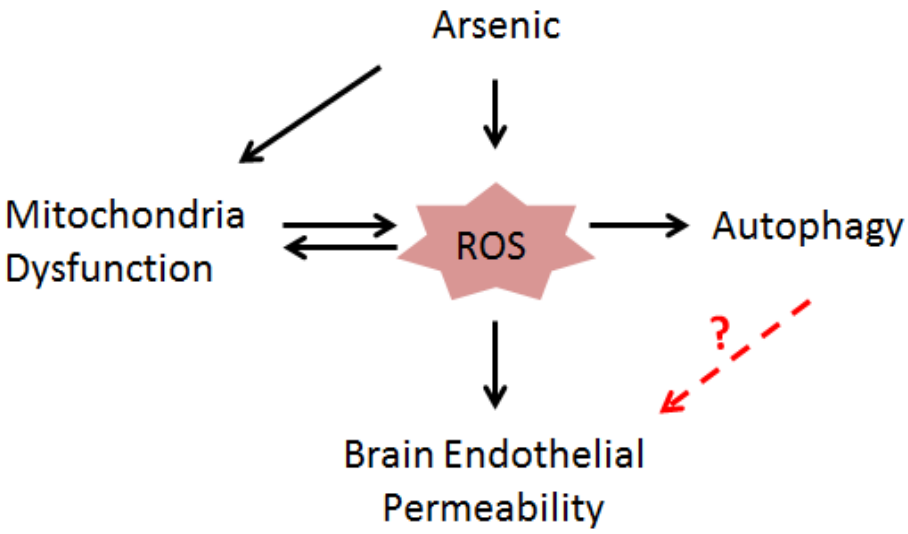

Figure 4.1 The mechanism of arsenic toxicity in BECs

References

1. Tolins, M., M. Ruchirawat, and P. Landrigan, *The Developmental Neurotoxicity of Arsenic: Cognitive and Behavioral Consequences of Early Life Exposure.* Annals of Global Health, 2014. **80**(4): p. 303-314.

2. Daneman, R. and A. Prat, *The blood-brain barrier.* Cold Spring Harb Perspect Biol, 2015. **7**(1): p. a020412.

3. Bao, L. and H. Shi, *Arsenite induces endothelial cell permeability increase through a reactive oxygen species-vascular endothelial growth factor pathway.* Chem Res Toxicol, 2010. **23**(11): p. 1726-34.

4. Patella, F., et al., *In-Depth Proteomics Identifies a Role for Autophagy in Controlling Reactive Oxygen Species Mediated Endothelial Permeability.* J Proteome Res, 2016. **15**(7): p. 2187-97.

5. Watanabe, T. and S. Hirano, *Metabolism of arsenic and its toxicological relevance.* Arch Toxicol, 2013. **87**(6): p. 969-79.

6. Rosado, J.L., et al., *Arsenic exposure and cognitive performance in Mexican schoolchildren.* Environ Health Perspect, 2007. **115**(9): p. 1371-5.

7. Registry, A.f.T.S.a.D., *Substance Priority List (SPL) Resource Page*. 2017.

8. Chung, J.Y., S.D. Yu, and Y.S. Hong, *Environmental source of arsenic exposure.* J Prev Med Public Health, 2014. **47**(5): p. 253-7.

9. Hughes, M.F., et al., *Arsenic exposure and toxicology: a historical perspective.* Toxicol Sci, 2011. **123**(2): p. 305-32.

10. *WHO fact sheet*, in *WHO*. 2017.

11. Tyler, C.R. and A.M. Allan, *The Effects of Arsenic Exposure on Neurological and Cognitive Dysfunction in Human and Rodent Studies: A Review.* Current Environmental Health Reports, 2014. **1**(2): p. 132-147.

12. Martinez-Finley, E.J., A.M. Ali, and A.M. Allan, *Learning deficits in C57BL/6J mice following perinatal arsenic exposure: consequence of lower corticosterone receptor levels?* Pharmacol Biochem Behav, 2009. **94**(2): p. 271-7.

13. Jing, J., et al., *Changes in the synaptic structure of hippocampal neurons and impairment of spatial memory in a rat model caused by chronic arsenite exposure.* Neurotoxicology, 2012. **33**(5): p. 1230-8.

14. Wasserman, G.A., et al., *Water arsenic exposure and children's intellectual function in Araihazar, Bangladesh.* Environ Health Perspect, 2004. **112**(13): p. 1329-33.

15. O'Bryant, S.E., et al., *Long-term low-level arsenic exposure is associated with poorer neuropsychological functioning: a Project FRONTIER study.* Int J Environ Res Public Health, 2011. **8**(3): p. 861-74.

16. Sen, D. and P. Sarathi Biswas, *Arsenicosis: Is it a Protective or Predisposing Factor for Mental Illness?* Iran J Psychiatry, 2012. **7**(4): p. 180-3.

17. Calderón, J., et al., *Exposure to Arsenic and Lead and Neuropsychological Development in Mexican Children.* Environmental Research, 2001. **85**(2): p. 69-76.

18. Roy, A., et al., *Association between arsenic exposure and behavior among first-graders from Torreon, Mexico.* Environ Res, 2011. **111**(5): p. 670-6.

19. Lisabeth, L.D., et al., *Arsenic in drinking water and stroke hospitalizations in Michigan.* Stroke, 2010. **41**(11): p. 2499-504.

20. Stamatovic, S.M., R.F. Keep, and A.V. Andjelkovic, *Brain endothelial cell-cell junctions: how to "open" the blood brain barrier.* Curr Neuropharmacol, 2008. **6**(3): p. 179-92.

21. Schoknecht, K. and H. Shalev, *Blood-brain barrier dysfunction in brain diseases: clinical experience.* Epilepsia, 2012. **53 Suppl 6**: p. 7-13.

22. Rai, A., et al., *Characterization of developmental neurotoxicity of As, Cd, and Pb mixture: synergistic action of metal mixture in glial and neuronal functions.* Toxicol Sci, 2010. **118**(2): p. 586-601.

23. Lopez-Ramirez, M.A., et al., *Role of caspases in cytokine-induced barrier breakdown in human brain endothelial cells.* J Immunol, 2012. **189**(6): p. 3130-9.

24. Daneman, R. and A. Prat, *The Blood–Brain Barrier.* Cold Spring Harbor Perspectives in Biology, 2015. **7**(1): p. a020412.

25.Tseng, W.P., *Effects and dose--response relationships of skin cancer and blackfoot disease with arsenic.* Environ Health Perspect, 1977. **19**: p. 109-19.

26. Yu, H.S., et al., *Studies on blackfoot disease and chronic arsenism in southern Taiwan: with special reference to skin lesions and fluorescent substances.* J Dermatol, 1984. **11**(4): p. 361-70.

27. Wu, M.M., et al., *Dose-response relation between arsenic concentration in well water and mortality from cancers and vascular diseases.* Am J Epidemiol, 1989. **130**(6): p. 1123-32.

28. Chen, C.J., et al., *Cancer potential in liver, lung, bladder and kidney due to ingested inorganic arsenic in drinking water.* Br J Cancer, 1992. **66**(5): p. 888-92.

29. Ellinsworth, D.C., *Arsenic, Reactive Oxygen, and Endothelial Dysfunction.* Journal of Pharmacology and Experimental Therapeutics, 2015. **353**(3): p. 458.

30. Tyler, C.R. and A.M. Allan, *The Effects of Arsenic Exposure on Neurological and Cognitive Dysfunction in Human and Rodent Studies: A Review.* Curr Environ Health Rep, 2014. **1**: p. 132-147.

31. Prakash, C., M. Soni, and V. Kumar, *Mitochondrial oxidative stress and dysfunction in arsenic neurotoxicity: A review.* J Appl Toxicol, 2016. **36**(2): p. 179-88.

32. Birben, E., et al., *Oxidative stress and antioxidant defense.* World Allergy Organ J, 2012. **5**(1): p. 9-19.

33. Halliwell, B., *Role of free radicals in the neurodegenerative diseases: therapeutic implications for antioxidant treatment.* Drugs Aging, 2001. **18**(9): p. 685-716.

34. Di Meo, S., et al., *Role of ROS and RNS Sources in Physiological and Pathological Conditions.* Oxid Med Cell Longev, 2016. **2016**: p. 1245049.

35. Lochhead, J.J., et al., *Oxidative stress increases blood-brain barrier permeability and induces alterations in occludin during hypoxia-reoxygenation.* J Cereb Blood Flow Metab, 2010. **30**(9): p. 1625-36.

36. Pun, P.B., J. Lu, and S. Moochhala, *Involvement of ROS in BBB dysfunction.* Free Radic Res, 2009. **43**(4): p. 348-64.

37. Tayarani, I., et al., *Enzymatic protection against peroxidative damage in isolated brain capillaries.* J Neurochem, 1987. **48**(5): p. 1399-402.

38. Scott, G.S., et al., *Glutamate-stimulated peroxynitrite production in a brain-derived endothelial cell line is dependent on N-methyl-d-aspartate (NMDA) receptor activation.* Biochemical Pharmacology, 2007. **73**(2): p. 228-236.

39. Freeman, L.R. and J.N. Keller, *Oxidative stress and cerebral endothelial cells: Regulation of the blood–brain-barrier and antioxidant based interventions.* Biochimica et Biophysica Acta (BBA) - Molecular Basis of Disease, 2012. **1822**(5): p. 822-829.

40. Boveris, A. and B. Chance, *The mitochondrial generation of hydrogen peroxide. General properties and effect of hyperbaric oxygen.* Biochem J, 1973. **134**(3): p. 707-16.

41. Murphy, M.P., *How mitochondria produce reactive oxygen species.* Biochem J, 2009. **417**(1): p. 1-13.

42. Paradies, G., et al., *Oxidative stress, mitochondrial bioenergetics, and cardiolipin in aging.* Free Radic Biol Med, 2010. **48**(10): p. 1286-95.

43. Leite, A.C., et al., *Mitochondria generated nitric oxide protects against permeability transition via formation of membrane protein S-nitrosothiols.* Biochim Biophys Acta, 2010. **1797**(6-7): p. 1210-6.

44. Giulivi, C., K. Kato, and C.E. Cooper, *Nitric oxide regulation of mitochondrial oxygen consumption I: cellular physiology.* Am J Physiol Cell Physiol, 2006. **291**(6): p. C1225-31.

45. Zhao, H., et al., *Superoxide reacts with hydroethidine but forms a fluorescent product that is distinctly different from ethidium: potential implications in intracellular fluorescence detection of superoxide.* Free Radic Biol Med, 2003. **34**(11): p. 1359-68.

46. Dikalov, S.I. and D.G. Harrison, *Methods for Detection of Mitochondrial and Cellular Reactive Oxygen Species.* Antioxidants & Redox Signaling, 2014. **20**(2): p. 372-382.

47. Cheng, G., et al., *Detection of mitochondria-generated reactive oxygen species in cells using multiple probes and methods: Potentials, pitfalls, and the future.* J Biol Chem, 2018.

48. Dikalova, A.E., et al., *Therapeutic targeting of mitochondrial superoxide in hypertension.* Circ Res, 2010. **107**(1): p. 106-16.

49. Spasojevic, I., *Free radicals and antioxidants at a glance using EPR spectroscopy.* Crit Rev Clin Lab Sci, 2011. **48**(3): p. 114-42.

50. Mrakic-Sposta, S., et al., *A Quantitative Method to Monitor Reactive Oxygen Species Production by Electron Paramagnetic Resonance in Physiological and Pathological Conditions*. Vol. 2014. 2014. 306179.

51. Fang, D., et al., *Increased Electron Paramagnetic Resonance Signal Correlates with Mitochondrial Dysfunction and Oxidative Stress in an Alzheimer's disease Mouse Brain.* J Alzheimers Dis, 2016. **51**(2): p. 571-80.

52. Ranguelova, D.K., *EPR SPECTROSCOPY - Bringing EPR to a Wider World: Biological ROS & RNS Detection*, in *Drug Development and Delivery*. 2018.

53. Fries, G.R. and F. Kapczinski, *N-acetylcysteine as a mitochondrial enhancer: a new class of psychoactive drugs?* Rev Bras Psiquiatr, 2011. **33**(4): p. 321-2.

54. Atkuri, K.R., et al., *N-Acetylcysteine—a safe antidote for cysteine/glutathione deficiency.* Current Opinion in Pharmacology, 2007. **7**(4): p. 355-359.

55. Saleh, A.A.S., *Anti-neuroinflammatory and antioxidant effects of N-acetyl cysteine in long-term consumption of artificial sweetener aspartame in the rat cerebral cortex.* The Journal of Basic & Applied Zoology, 2015. **72**: p. 73-80.

56. Wilcox, C.S., *Effects of tempol and redox-cycling nitroxides in models of oxidative stress.* Pharmacol Ther, 2010. **126**(2): p. 119-45.

57. Batinic-Haberle, I., J.S. Reboucas, and I. Spasojevic, *Superoxide dismutase mimics: chemistry, pharmacology, and therapeutic potential.* Antioxid Redox Signal, 2010. **13**(6): p. 877-918.

58. Francischetti, I.M.B., et al., *Tempol, an Intracellular Antioxidant, Inhibits Tissue Factor Expression, Attenuates Dendritic Cell Function, and Is Partially Protective in a Murine Model of Cerebral Malaria.* PLoS ONE, 2014. **9**(2): p. e87140.

59. Monti, E., et al., *Nitroxide TEMPOL impairs mitochondrial function and induces apoptosis in HL60 cells.* J Cell Biochem, 2001. **82**(2): p. 271-6.

60. Januschowski, K., et al., *Investigating retinal toxicity of tempol in a model of isolated and perfused bovine retina.* Graefes Arch Clin Exp Ophthalmol, 2014. **252**(6): p. 935-41.

61. Qi, Y., et al., *Autophagy in arsenic carcinogenesis.* Experimental and Toxicologic Pathology, 2014. **66**(4): p. 163-168.

62. Zhang, Z., R. Singh, and M. Aschner, *Methods for the Detection of Autophagy in Mammalian Cells.* Curr Protoc Toxicol, 2016. **69**: p. 20.12.1-20.12.26.

63. Zhang, Z., R. Singh, and M. Aschner, *Methods for the Detection of Autophagy in Mammalian Cells.* Current protocols in toxicology / editorial board, Mahin D. Maines (editor-in-chief) ... [et al.], 2016. **69**: p. 20.12.1-20.12.26.

64. Fonseca, A.C., et al., *Loss of proteostasis induced by amyloid beta peptide in brain endothelial cells.* Biochim Biophys Acta, 2014. **1843**(6): p. 1150-61.

65. Cheng, Y., et al., *Therapeutic Targeting of Autophagy in Disease: Biology and Pharmacology.* Pharmacological Reviews, 2013. **65**(4): p. 1162.

66. Wu, Y.T., et al., *Dual role of 3-methyladenine in modulation of autophagy via different temporal patterns of inhibition on class I and III phosphoinositide 3-kinase.* J Biol Chem, 2010. **285**(14): p. 10850-61.

67. Slavin, S.A., et al., *Autophagy inhibitor 3-methyladenine protects against endothelial cell barrier dysfunction in acute lung injury.* Am J Physiol Lung Cell Mol Physiol, 2018. **314**(3): p. L388-l396.

68. Ni, H., et al., *Autophagy inhibitor 3-methyladenine regulates the expression of LC3, Beclin-1 and ZnTs in rat cerebral cortex following recurrent neonatal seizures.* World Journal of Emergency Medicine, 2010. **1**(3): p. 216-223.

69. Ito, S., et al., *3-Methyladenine suppresses cell migration and invasion of HT1080 fibrosarcoma cells through inhibiting phosphoinositide 3-kinases independently of autophagy inhibition.* Int J Oncol, 2007. **31**(2): p. 261-8.

70. Kiššová, I., et al., *Lipid oxidation and autophagy in yeast.* Free Radical Biology and Medicine, 2006. **41**(11): p. 1655-1661.

71. Chen, Y., M.B. Azad, and S.B. Gibson, *Superoxide is the major reactive oxygen species regulating autophagy.* Cell Death And Differentiation, 2009. **16**: p. 1040.

72. Lee, J., S. Giordano, and J. Zhang, *Autophagy, mitochondria and oxidative stress: cross-talk and redox signalling.* Biochemical Journal, 2012. **441**(Pt 2): p. 523-540.

73. Domigan, C.K., et al., *Autocrine VEGF maintains endothelial survival through regulation of metabolism and autophagy.* J Cell Sci, 2015. **128**(12): p. 2236-48.

74. Wang, Q., et al., *2-Deoxy-D-glucose treatment of endothelial cells induces autophagy by reactive oxygen species-mediated activation of the AMP-activated protein kinase.* PLoS One, 2011. **6**(2): p. e17234.

75. Chen, L., B. Zhang, and M. Toborek, *AUTOPHAGY IS INVOLVED IN NANOALUMINA-INDUCED CEREBROVASCULAR TOXICITY.* Nanomedicine : nanotechnology, biology, and medicine, 2013. **9**(2): p. 212-221.

76. Chen, H.-R., et al., *Macrophage migration inhibitory factor induces vascular leakage via autophagy.* Biology Open, 2015. **4**(2): p. 244-252.

77. Escudero-Lourdes, C., *Toxicity mechanisms of arsenic that are shared with neurodegenerative diseases and cognitive impairment: Role of oxidative stress and inflammatory responses.* Neurotoxicology, 2016. **53**: p. 223-235.

78. Campos-Bedolla, P., et al., *Role of the blood-brain barrier in the nutrition of the central nervous system.* Arch Med Res, 2014. **45**(8): p. 610-38.

79. Abbott, N.J., *Blood-brain barrier structure and function and the challenges for CNS drug delivery.* J Inherit Metab Dis, 2013. **36**(3): p. 437-49.

80. Rosenberg, G.A., *Neurological diseases in relation to the blood-brain barrier.* J Cereb Blood Flow Metab, 2012. **32**(7): p. 1139-51.

81. Ellinsworth, D.C., *Arsenic, reactive oxygen, and endothelial dysfunction.* J Pharmacol Exp Ther, 2015. **353**(3): p. 458-64.

82. Tsai, M.H., et al., *A mouse model for the study of vascular permeability changes induced by arsenic.* Toxicol Mech Methods, 2005. **15**(6): p. 433-7.

83. Yan, J., Z. Zhang, and H. Shi, *HIF-1 is involved in high glucose-induced paracellular permeability of brain endothelial cells.* Cell Mol Life Sci, 2012. **69**(1): p. 115-28.

84. Thomas, V.C., et al., *Electron Paramagnetic Resonance (EPR) Spectroscopy to Detect Reactive Oxygen Species in Staphylococcus aureus.* Bio Protoc, 2015. **5**(17).

85. Kurdi, M., et al., *Depletion of Cellular Glutathione modulates LIF-Induced JAK1-STAT3 Signaling in Cardiac Myocytes*. 2012.

86. Han, Z., et al., *Mitochondria-Derived Reactive Oxygen Species Mediate Heme Oxygenase-1 Expression in Sheared Endothelial Cells.* Journal of Pharmacology and Experimental Therapeutics, 2009. **329**(1): p. 94.

87. Han, Y.H., et al., *Effects of arsenic trioxide on cell death, reactive oxygen species and glutathione levels in different cell types.* Int J Mol Med, 2010. **25**(1): p. 121-8.

88. Guan, Y., et al., *Celastrol attenuates oxidative stress in the skeletal muscle of diabetic rats by regulating the AMPK-PGC1alpha-SIRT3 signaling pathway.* Int J Mol Med, 2016. **37**(5): p. 1229-38.

89. Wang, S., et al., *[Effects of autophagy on lipopolysaccharide-induced vascular hyper-permeability].* Zhonghua Wei Zhong Bing Ji Jiu Yi Xue, 2016. **28**(8): p. 673-7.

90. Xu, D., et al., *Inhibition of autophagy ameliorates pulmonary microvascular dilation and PMVECs excessive proliferation in rat experimental hepatopulmonary syndrome.* Sci Rep, 2016. **6**: p. 30833.

91. Mizushima, N. and T. Yoshimori, *How to Interpret LC3 Immunoblotting.* Autophagy, 2007. **3**(6): p. 542-545.

92. Tran, A.T., et al., *Autophagy Inhibitor 3-Methyladenine Potentiates Apoptosis induced by Dietary Tocotrienols in Breast Cancer Cells.* European journal of nutrition, 2015. **54**(2): p. 265-272.

93. Luo, J. and W. Shu, *15 - Arsenic-Induced Developmental Neurotoxicity*, in *Handbook of Arsenic Toxicology*, S.J.S. Flora, Editor. 2015, Academic Press: Oxford. p. 363-386.

94. Monaghan-Benson, E. and E.S. Wittchen, *In vitro analyses of endothelial cell permeability.* Methods Mol Biol, 2011. **763**: p. 281-90.

95. Gastfriend, B.D., S.P. Palecek, and E.V. Shusta, *Modeling the blood–brain barrier: Beyond the endothelial cells.* Current Opinion in Biomedical Engineering, 2018. **5**: p. 6-12.

96. Zhang, Z., et al., *Role of reactive oxygen species in arsenic-induced transformation of human lung bronchial epithelial (BEAS-2B) cells.* Biochem Biophys Res Commun, 2015. **456**(2): p. 643-8.

97. Kim, H.K., et al., *Reactive oxygen species (ROS) play an important role in a rat model of neuropathic pain.* Pain, 2004. **111**(1-2): p. 116-24.

98. Pace, C., R. Dagda, and J. Angermann, *Antioxidants Protect against Arsenic Induced Mitochondrial Cardio-Toxicity.* Toxics, 2017. **5**(4).

99. Sun, S.-Y., *N-acetylcysteine, reactive oxygen species and beyond.* Cancer biology & therapy, 2010. **9**(2): p. 109-110.

100. Beltrán, B., et al., *The effect of nitric oxide on cell respiration: A key to understanding its role in cell survival or death.* Proceedings of the National Academy of Sciences, 2000. **97**(26): p. 14602.

101. Yorimitsu, T. and D.J. Klionsky, *Autophagy: molecular machinery for self-eating.* Cell Death And Differentiation, 2005. **12**: p. 1542.

102. Jiang, F., *Autophagy in vascular endothelial cells.* Clinical and Experimental Pharmacology and Physiology, 2016. **43**(11): p. 1021-1028.

103. Du, J., et al., *Role of autophagy in angiogenesis in aortic endothelial cells.* American Journal of Physiology-Cell Physiology, 2011. **302**(2): p. C383-C391.

104. Samanta, S., et al., *Abstract 13299: Cross Talk Between Hyper Permeability and Autophagy in Endothelial Cells With Persistent Inflammation.* Circulation, 2016. **134**(Suppl 1): p. A13299.

105. McAfee, Q., et al., *Autophagy inhibitor Lys05 has single-agent antitumor activity and reproduces the phenotype of a genetic autophagy deficiency.* Proc Natl Acad Sci U S A, 2012. **109**(21): p. 8253-8.

106. Yang, Y.P., et al., *Application and interpretation of current autophagy inhibitors and activators.* Acta Pharmacol Sin, 2013. **34**(5): p. 625-35.

107. Bates, D.O., *Vascular Endothelial Growth Factors and vascular permeability.* Cardiovascular research, 2010. **87**(2): p. 262-271.

108. Wang, W., W.L. Dentler, and R.T. Borchardt, *VEGF increases BMEC monolayer permeability by affecting occludin expression and tight junction assembly.* Am J Physiol Heart Circ Physiol, 2001. **280**(1): p. H434-40.

109. Li, R., et al., *Manipulation of autophagy: a novelly potential therapeutic strategy for retinal neovascularization.* BMC Ophthalmology, 2018. **18**(1): p. 110.

110. An, Y., et al., *Autophagy promotes MSC-mediated vascularization in cutaneous wound healing via regulation of VEGF secretion.* Cell Death & Disease, 2018. **9**(2): p. 58.

111. Du, J., et al., *Role of autophagy in angiogenesis in aortic endothelial cells.* Am J Physiol Cell Physiol, 2012. **302**(2): p. C383-91.